HHS Public Access

Author manuscript

Phytother Res. Author manuscript; available in PMC 2021 September 01.

Published in final edited form as:

Phytother Res. 2020 September ; 34(9): 2366–2384. doi:10.1002/ptr.6687.

Neferine, an alkaloid from lotus seed embryo target HeLa and SiHa cervical cancer cells via pro-oxidant anticancer mechanism

Subramanyam Dasari[1,#], **Velavan Bakthavachalam**[1,#], **Somaiah Chinnapaka**[1], **Reshmii Venkatesan**[1], **Angela Lincy Prem Antony Samy**[1], **Gnanasekar Munirathiknam**[1,*]

[1]Department of Biomedical Sciences, College of Medicine, University of Illinois, Rockford, IL

Abstract

Apoptosis and autophagy are important processes that control cellular homeostasis and have been highlighted as promising targets for novel anticancer drugs. This study aims to investigate the inhibitory effects and mechanisms of Neferine (Nef), an alkaloid from the lotus seed embryos of *Nelumbo nucifera*, as a dual inducer of apoptosis and autophagy through the ROS activation in cervical cancer cells. Nef and *N. nucifera* extract suppressed the cell viability of HeLa and SiHa cells in a dose dependent manner. Importantly, Nef showed minimal toxicity to normal cells. Furthermore, Nef inhibited anchorage-independent growth, colony formation and migration ability of cervical cancer cells. Nef induces mitochondrial apoptosis by increasing pro-apoptotic protein bax, cytosolic cytochrome-C, cleaved caspase-3 and −9, poly ADP ribose polymerase (PARP) cleavage, DNA damage (pH_2AX) while down regulating Bcl-2, pro-caspase-3 and −9 and TCTP. Of note, apoptotic effect by Nef was significantly attenuated in the presence of N-acetylcysteine (NAC), suggesting pro-oxidant activity of this compound. Nef also promoted autophagy induction through increasing beclin-1, atg-4, −5 and −12, LC-3 activation and P62/SQSTM1 as determined by Western blot analysis. Collectively, these results demonstrate that Nef is a potent anticancer compound against cervical cancer cells through inducing apoptosis and autophagic pathway involving ROS.

Keywords

Cervical cancer; Neferine; reactive oxygen species; apoptosis and autophagy; DNA damage

1. Introduction

Cervical cancer is the second leading cause of cancer death in women aged 20 to 39 years in the USA and 4th most common cancer among women worldwide. According to Cancer Statistics, 2020, it is estimated that 13,800 new cases of cervical cancer and 4,290 related deaths in the USA, in which most cases are squamous cell carcinoma followed by adenocarcinoma (Siegel et al., 2020). Clinical, epidemiological, and molecular studies

*Address for correspondence: Dr. Gnanasekar Munirathinam, Department of Biomedical Sciences, University of Illinois College of Medicine, 1601 Parkview Avenue, Rockford, IL, 61107. Telephone: 815-395-5773. mgnanas@uic.edu.
#:contributed equally to this study and both need to be considered as first authors

Conflict of interest

The authors declare that they do not have conflicts of interest.

support that persistent infections with high-risk types of human papillomavirus (HPV) are essential in the development of cervical cancer (Zur Hausen, 2008). The most common HPV genotypes in patients with invasive cervical cancer are 16, 18, 31, 33, 35, 45, 52, and 58 (Zur Hausen, 2008). Although surgery and chemoradiotherapy can cure 80–95% of women with cervical intraepithelial neoplasia (CIN), an early stage cancer (Peralta-Zaragoza et al., 2012), the recurrent and metastatic disease remains a major cause of cancer morbidity and mortality for the vast majority of patients with cervical cancer. The uncontrolled proliferation and migration of cancer cells are the important steps of cervical cancer metastasis (Li and Wu, 2016). Many efforts have been made to design new drugs and develop gene therapies to treat cervical cancer. Patients undergoing current treatment strategies suffer from various undesirable side effects and develop cancer that is more lethal. Various studies suggest that the therapeutic potential of natural compounds might be an effective alternative for treatment of cervical cancer. Bioactive compounds from plants have led to the development of treatment modalities for different ailments in modern medicine, including cancer.

Natural products have played a significant role in the discovery of anticancer drugs; more than 60% of anticancer drugs are of natural origin (Newman and Cragg, 2016; Singh et al., 2016). Neferine (Nef) is a bisbenzylisoquinoline alkaloid, present in the family Nelumbonaceae, which is a major alkaloid found in the seed embryo of lotus (*Nelumbo nucifera*) Figure 1A (Liu et al., 2009; Poornima et al., 2014; Asokan et al., 2018). *N. nucifera* have been used for various medicinal purposes in various systems of medicine including folk medicine, Ayurveda, Chinese traditional medicine, and oriental medicine. Many chemical constituents have been isolated from *N. nucifera* including Liensinine, Isoliensinine, Neferine, Pronuciferine and Rutin (Paudel and Panth, 2015). Previous studies have shown that Nef has several pharmacological actions, including inhibition of the proliferation of vascular smooth muscle cells (VSMCs), hypertrophic scar fibroblasts (Li et al., 2010), and diabetes (Guan et al., 2014). Interestingly, it exhibits the reversal of multi-drug resistance in cancer cells (Kadioglu et al., 2017). Nef was also shown to inhibit pyroptosis in kidney cells (Tang et al., 2019) and has been suggested to provide protection against cell death in muscle cells, cardiovascular diseases, and neurological diseases (Baskaran et al., 2016; Manogaran et al., 2019). In case of cancer, Nef was demonstrated to induce ROS dependent mitochondrial mediated apoptosis in liver, lung, breast, cervical and osteosarcoma cancer cells (Poornima et al., 2013a; Poornima et al., 2013b, Yang et al.,2016, Zhang et al., 2011; Eid et al., 2017). Although previous studies have reported Nef regulated autophagy and apoptosis mediated cell death involving ROS in cancers such as lung, ovarian cancer and neuroblastoma (Poornima et al., 2013; Xu et al., 2016; Pham et al., 2018), the exact anti-cancer mechanism of Nef is yet to be clearly defined. ROS play an important role in cell survival, cell death and in the maintenance of the cellular homeostasis. Atg4 is a ROS regulated cysteine protease, which play an important role in oxidative stress induced autophagy related cell death (Scherz-Shouval et al., 2007). In this study, we show that Nef upregulates Atg4 via ROS to induce autophagy with concomitant activation of apoptosis by modulating Bax and Bcl-2 levels in HeLa and SiHa cervical cancer cells. Furthermore, we provide experimental evidence to demonstrate the therapeutic effects of Nef using HeLa and SiHa cells as *in vitro* model of cervical cancer as representative of the papillomavirus (HPV) types 18 and 16 driven cervical cancers respectively.

2. Materials and methods

2.1 Chemicals and antibodies

Eagle's Minimum Essential Medium (MEM), fetal bovine serum and Lipofectamine2000 were purchased from Thermo Scientific, USA. Neferine (purity ≥98%) and 3–4,5-dimethylthiazol-2-yl,2,5-diphenyltetrazoliumbromide (MTT), N-acetyl cysteine (NAC), Propidium Iodide (PI), 3-methyladenine, (3MA), 2′,7′-Dichlorofluorescin diacetate (DCFH2-DA) and monodansylcadaverine (MDC) was procured from Sigma Aldrich, USA. *Nelubo nucifera* dried seed liquid extract (Herbal Terra, USA). Antibodies against bcl-2, TCTP, caspase-3 & 9, cleaved caspase-3 & 9, PARP, pH2AX, beclin-1, LC-3, atg-4, 5 & 12, P62/SQSTM1, HRP conjugated anti-rabbit and anti-mouse antibodies were obtained from Cell Signaling Technology (Danvers, MA, USA). The following reagents were obtained from the respective manufacturers as indicated in brackets: Cytochrome-c antibody (Bioss), bax antibody (ebioscience), caspase inhibitor Z-VAD-FMK (APExBIO), Annexin V-FITC (BD biosciene), caspase-3 ELISA kit (R&D system, Inc, USA). EGFP-LC3 was a gift from Karla Kirkegaard (Addgene plasmid # 11546) and all other chemicals used were of analytical grade.

2.2. Cell lines and cell culture

HeLa, SiHa, and HEK-293 cell lines were obtained from ATCC, USA. HeLa and SiHa cell lines were derived from female cervix, morphologically they are epithelial cells derived from the adenocarcinoma and squamous cell carcinoma respectively. HEK-293 cells were isolated from normal human embryonic kidney cells. These cells were grown to confluence in 25-ml flasks supplemented with Eagle's Minimum Essential Medium and grown in 10% fetal bovine serum (FBS) (v/v), 30 μg/ml antimycotic and 20 μg /ml gentamycin in a 5% of CO_2 incubator. Cells at 50–60% confluence were used for all the assays.

2.3 Cell proliferation assay

Cell viability was determined by the MTT (3-(4, 5-dimethylthiazol-2-yl)-2,5-diphenyltetrazolium bromide) assay. HeLa, SiHa and HEK-293 cells were seeded at a density of 1×10^5 cells/well in 96-well plate and were allowed to incubate at 37°C and 5% CO_2 incubator until the cell confluence reached to 50% for treatment. Then the cells were treated with various concentrations of Nef (5, 10, 25 and 50 μM/ml) and *N. nucifera* (1, 5, 10, 25, 50, 100, 250, 500, 750 and 1000μg/ml) and incubated for 48hrs. At the end of the treatment, 10 μl of MTT dye (5mg/ml) to each well was added and incubated at 37°C for 4 hrs. Then the media with MTT was removed, the purple formazan crystals were dissolved in 100μl of MTT solubilizing solution (90% Isopropanol +10% Triton X-100) and the absorbance was measured at 570 nm using a BIO-RAD microplate reader model 680. To evaluate the anticancer mechanism, cervical cancer cells, were treated with Nef in presence or absence of caspase inhibitor (Z-VAD-FMK), an antioxidant N-acetyl cysteine (NAC) and autophagy inhibitor, 3-Methyladenine (3 MA) respectively as reported previously (Dasari et al., 2018a).

2.4 Anchorage-independent growth assay/Soft agar assay

The anti-cancer effect of Nef on both HeLa and SiHa cells was determined by soft agar assay. Cells ($15–20\times10^3$) were mixed with 0.7% agarose (Soft agarose) solution in complete MEM with 20% FBS and poured on top of solidified base agar (1%) in 6 well plates. The soft agarose also mixed with various concentrations of Nef along with one control well. Feed the cells with complete MEM containing 20% FBS for every 4 days up to 4–5 weeks. After incubation period, the colonies were stained with 200 μl of 0.005% crystal violet and analyzed the number of colonies using Microscope (Dasari et al., 2018a).

2.5 Colony formation assay

Clonogenic assay was performed to check the effect of Nef on cervical cancer cell lines (HeLa and SiHa). Colony formation assay was performed based on the protocol by Chinnapaka et al., 2019. Briefly, 500 cells/well were seeded onto 6-well in MEM with 10% FBS. After 24hrs, cervical cancer cells were treated with varying concentrations of Nef with or without inhibitors (2.5mM NAC or 25μ MCI). Media change was done for every 4 days with fresh media contains Nef with or without inhibitors until proper colony formation. Following this, colonies were fixed with acetic acid: methanol (1:7) for 5 minutes and stained with crystal violet (0.005%) for 2–3 hrs and washed with distilled water. Colonies were air dried for 3 to 4 days and colonies were counted, and images were documented.

2.6 Migration Assay

Migration assay was performed as described previously by Gheewala et al., 2018. Briefly, Cervical cancer (HeLa and SiHa) cells (1×10^5) were seeded in 24 well, 6.5-mm-internal-diameter transwell plates (8.0 μm pore size; Corning, USA) 200 μl serum free RPMI medium containing different concentration of Nef (10, 25 and 50μM) and seeded into the upper well of Transwell chamber, and the lower chamber was filled with 500μl of RPMI containing 10% FBS. The chambers were incubated at 37˚C, and cells were allowed to migrate for 48hrs. After migration, non-migrated cells on the upper surface of the filters were wiped off using a cotton swab and migrated cells were fixed with 4% paraformaldehyde and stained with 0.5% crystal violet. Then migrated cells were imaged under a microscope (Olympus1X73).

2.7 Measurement of Reactive oxygen species (ROS)

Intracellular ROS production was measured by a fluorescent dye 2′,7′-dichlorofluorescin diacetate (DCFH2-DA) induced by Nef using previously described by Chinnapaka et al., 2019. In brief, cervical cancer cells (2×10^4cells/500μl) were cultured in an 8-chamber culture slide (FALCON), and treated with various concentrations of Nef (0, 5, 10, 25 and 50 μM) and incubated at 37°C, 5% CO_2 for a period of 2–6 hrs. After treatment, cells were washed with PBS and incubated with 10μM DCFH2-DA dye suspended in serum free MEM for 30 minutes at 37 °C. Finally, the cells were washed with PBS and observe under fluorescent microscope, the quantification of the fluorescence was measured by using image J software (Dasari et al., 2018b).

2.8 Detection of Apoptosis by Annexin V-FITC Staining

Apoptotic cell morphology was detected by Annexin V-FITC kit (BioVision Inc), in which 2×10^4cells/500µl of MEM were cultured on 8-well chamber slide and treated with various concentrations of Nef. After the incubation period (48 hrs), cells were stained with 5µl of Annexin V-FITC and 5µl of propidium iodide (PI) dissolved in 500µl of 1X binding buffer per each well and incubated in dark at room temperature (RT) for 10 minutes. Then, cells were washed with PBS and imaged the apoptotic cell morphology under a fluorescence microscope (Dasari et al., 2018a).

2.9 Cell cycle analysis

Cell cycle analysis was quantified by flow cytometry analysis. After being treated with various concentrations of Nef (10, 25 and 50µM) for 48 hrs, the cells were harvested by trypsinization and collected by centrifugation. The cells were fixed with ice-cold ethanol (70% v/v) at 4°C overnight. After centrifugation, the fixed cells were rinsed twice with PBS and resuspended in 500µl PBS containing 50 µg/ml RNase (Invitrogen) and 5 µg/ml propidium iodide (Sigma-Aldrich) at room temperature for 30 minutes at dark. Cell cycle distribution was analyzed by measuring DNA content using flow cytometry (BD FACS Calibri, BD biosciences, USA).

2.10 Detection of DNA Apoptotic markers (pH_2AX, cleaved caspase-3, cytochrome-C) by Immunofluorescence

Immunofluorescence was performed based on our previous protocol (Shetty et al., 2016). Briefly, cervical cancer cells (HeLa and SiHa) were cultured on 8-chamber plates, treated with Nef (25µM), and incubated at 37°C and 5% CO_2 for 48 hrs. Following treatment cells were fixed (4% paraformaldehyde) for 15 minutes and blocked with 5% goat normal serum (Invitrogen) with 0.3% Triton X- 100 (Sigma–Aldrich) in PBS. Cells were washed (PBS) and incubated with primary antibodies to pH2AX (1:200), caspase-3 (1:200) and cytochrome c (1:200) respectively for overnight at 4°C. After three successive washings, cells were probed with 0.1µg/ml of secondary anti-mouse Ig-G or anti-rabbit Ig-G conjugated with FITC for 1 hr at RT. Cells were counter-stained with DAPI (30nM) for 10–15 minutes with PBS, and a coverslip with Fluorogel (Electron Microscopy Sciences, PA, USA) was prepared for visual inspection with an Olympus Fluoview laser scanning confocal microscope.

2.11 Assessment of active caspase-3 concentration

To assess the effect of Nef on apoptosis, the active caspase-3 level was measured by using quantitative caspase-3 ELISA kit (R&D Systems, Inc. USA). The protocol was followed according to Pan et al., 2016 with some modifications. In brief, cells were treated with various concentrations of Nef (10, 25, 50µM) and drug free media (control group) for 48 hrs. After incubation, cell extracts were prepared according to manufacturer's instructions. Cells were mixed with lysis buffer and cell lysates were transferred into the wells of a micro-plate pre-coated with a monoclonal antibody specific for caspase-3. Substrate solution (Streptavidin-HRP) was added to the wells. The enzyme reaction yielded a blue product that turned yellow when a stop solution was added. Optical density was determined within 30

minutes using a micro-plate reader set to 450nm with a wavelength correction at 540nm or 570nm. The active caspase-3 concentrations were calculated from a standard curve constructed with known concentrations of active caspase-3.

2.12 Detection of autophagy marker LC-3 by Immunofluorescence

LC-3 detection was performed based on previous study (Li et al., 2018). Briefly, cervical cancer cells were cultured on 8-chamber plates, treated with Nef and allowed to incubate at 37°C at 5% CO_2 for 48 hrs. After the treatment, the cells were fixed with 4% formaldehyde for 15 minutes and blocked with 5% goat normal serum (Invitrogen) with 0.3% Triton X-100 (Sigma–Aldrich). Then the cells were washed with PBS and incubated with primary antibodies LC-3 (1:200) for 1hr. After three successive washings, cells were treated with secondary anti-rabbit Ig-G conjugated with FITC for 1 hr. Finally, the cells were counter stained with DAPI (30nM) for 10 minutes and the wells were subsequently washed with PBS and prepare coverslip with Fluorogel (Electron Microscopy Sciences, Hatfield, PA, USA) for visual inspection with an Olympus Fluoview laser scanning confocal microscope.

2.13 Transient transfection with Green fluorescent protein (GFP)-light chain 3 B (LC3B) plasmid transfection and autophagy assays

Both HeLa and SiHa cells were cultured on 8 well chamber plates at a density of 2×10^4 cells/well up to 50% confluence. EGFP-LC3 plasmid DNA (2 μg/ml) was transiently transfected into the cells using Lipofectamine 2000 (Thermo Fisher Scientific) according to the manufacturer's protocol. EGFP-LC3 was a gift from Karla Kirkegaard (Addgene plasmid # 11546; http://n2t.net/addgene:11546; RRID: Addgene_11546). After incubation in Opti-MEM medium for 4–5 hrs, the cells were treated with Nef in MEM containing 10% FBS and allowed to incubate at 37°C at 5% CO_2 for 48 hrs. The formation of fluorescent puncta of autophagosomes were observed by using Olympus fluoview confocal microscopy (Hu et al., 2012).

2.14 Detection of autophagic vacuoles by Monodansylcadaverine (MDC) staining

To detect the autophagic vacuoles, a fluorescent dye known as monodansylcadaverine (MDC), was used as a specific marker for autophagic organelles (Yang et al., 2014). After the treatment, cells were washed with PBS and probed with MDC (100 μM) and allowed to incubate 15–30 minutes. For autophagy inhibitor analysis, cells were also treated with the combination of autophagy inhibitor 3-MA (2.5 mM) along with Nef (25 μM) and allowed to incubate for 48 hrs. After incubation, the cells were washed with PBS and analyzed by laser scanning confocal microscopy, Olympus fluoview FV10i.

2.15 Detection of autophagic vacuoles by LysoTracker staining

LysoTracker is a green fluorescent dye used for the detection of functional lysosomes released in response to autophagy induced by drugs. After the treatment cells were probed with LysoTracker (75 nM/ml) for 30 minutes at 37°C and the cells were then counterstained with DAPI for 10 minutes in the dark. Fluorescent micrographs images were taken using laser scanning confocal microscopy, Olympus fluoview FV10i (Liu et al., 2013).

2.16 Quantitative expression of mRNA by Real Time-qPCR analysis

HeLa and SiHa cells were treated with different concentrations of Nef (10, 25 and 50μM) for 48 hrs. The cells were harvested, and total RNA was extracted using Trizol reagent (Invitrogen, USA) according to the standard protocol (Chinnapaka et al., 2019). Complementary DNA (cDNA) was synthesized using high capacity cDNA reverse transcription kit (Thermo Scientific, USA) by using Mastercycler PCR machine (Eppendorf, USA). Real-time PCR was performed using maxima SYBR green qPCR master mix (Thermo Scientific, USA). The expression of mRNA was quantified by real time PCR (QuantStudio 3, Applied Biosystems, CA, USA) by using the following thermocycling conditions: 95°C for 30 sec, followed by 40 cycles of 95°C for 5 sec and 60°C for 30 sec. The β-actin was used as an endogenous control (housekeeping gene). The Ct values were extracted by using the SDS-software (Applied Biosystems, Foster City, CA, USA) and the expression level of the housekeeping gene (β-actin) was used for normalization, fold changes were calculated with the $2^{-\Delta\Delta Ct}$ method.

The gene-specific primer pairs used in this study were as follows

bcl-2 (F) 5 ’ -GATTGTGGCCTTCTTTGAG-3 ’

bcl-2 (R) 5 ’ GTTCCACAAAGGCATCC-3 ’;

bax (F) 5 ’-AACTGGACAGTAACATGGAG-3 ’;

bax(R) 5 ’-TTGCTGGCAAAGTAGAAAAG-3 ’;

beclin-1(F)5 ’-CAGTATCAGAGAGAATACAGTG-3 ’

beclin-1(R)5 ’-TGGAAGGTTGCATTAAAGAC-3 ’;

LC-3 (F) 5 ’-AGAAAGGATTTTGAGGAGGG- 3 ’;

LC-3 (R) 5 ’-TTCATCTGCAAAACTGAGAC-3 ’.

HPV-E6 (F) 5 ’-AATACTATGGCGCGCTTTGA-3 ’;

HPV-E6 (R) 5 ’-CTGGATTCAACGGTTTCTGG-3 ’;

HPV-E7 (F) 5 ’-TGCATGGACCTAAGGCAA-3 ’;

HPV-E7 (R) 5 ’-GCTGGGATGCACACCA-3 ’;

β-actin (F) 5 ’-GACGACATGGAGAAAATCTG-3 ’;

β-actin (R) 5 ’-ATGATCTGGGTCATCTTCTC-3 ’.

2.17 Protein expression profiling using western blot analysis

After Nef treatment, cervical cancer cells (HeLa and SiHa) were harvested and washed with PBS. Total cellular protein was isolated using lysis buffer (BD Bioscience). Protein concentration was determined using a protein (BCA method) assay kit (Pierce Chemicals,

USA). Equal amounts of protein (25–50 μg/lane) in Laemmli sample buffer (Bio-Rad) were loaded and electrophoresed on 10–12% SDS-PAGE and transferred to nitro cellulose membranes by semi-transfer method. The membranes were blocked with 5% skim milk and incubated with primary antibodies (1:1000). After washing with TBS-T, the membranes were incubated with corresponding HRP conjugated anti-mouse or anti-rabbit secondary antibodies followed by detection with enhanced chemiluminescence staining and develop the bands at X-ray film. β-actin was used to normalize protein loading (Dasari et al., 2018a).

2.18 Statistical analysis

All experiments were performed three times in triplicates. Results were expressed as mean ±SEM. Multiple comparisons were done using one-way ANOVA followed by Tukey's multiple comparison test, using SPSS 20 software (SPSS Inc, Chicago, IL). Differences were considered statistically significant when $P < 0.05$.

3. RESULTS

3.1 Nef inhibits growth and viability of cervical cancer cells

Cervical cancer cells (HeLa and SiHa) were treated with various concentrations of Nef (5, 10, 25 and 50μM) for 48hrs. Our results showed that Nef significantly inhibited cell proliferation *in vitro* in a dose-dependent manner (Figure 1B). Nef treatment inhibited the growth of cervical cancer cells by 50% at 25μM at 48hrs. Specifically, HeLa cells were found to be more sensitive than SiHa cells at 48hrs. Our results further showed that the anti-proliferative effects of Nef was abrogated in the presence of autophagy inhibitor 3 methyladenine (3-MA), caspase inhibitor Z-VAD-FMK and anti-oxidant N-acetyl cysteine (NAC) suggesting that autophagy and caspase activation as the underlying anti-cancer mechanism through the oxidative stress (Figure 1C). However, Nef showed minimal cytotoxic effects on normal kidney cells (HEK-293) up to 100μM for 48hrs treatment (Figure 1D). Furthermore, we have evaluated the effect of *N. nucifera* (seed crude extract) on HeLa and SiHa cells with different concentrations ranging from 1 μg/ml to 1mg/ml for 48hrs, the result indicates that crude extract displayed toxicity to cervical cancer cells at higher doses (Supplementary Figure 1A & B). As shown in Supplementary Figure 2, human cervical cancer cells (HeLa and SiHa) treated with Nef revealed morphological changes, cohesive clusters of well-shaped and smooth surface. In contrast, both the cell lines, with the treatment of Nef appeared to be shrunken, especially in HeLa cells. Nef suppresses colony formation of cervical cancer cells; anchorage-independent growth of cervical cancer (HeLa and SiHa) cells were determined by soft agar assay, in which untreated cells grew large colonies after 4–5 weeks of incubation. By contrast, there were no visible colonies observed in the presence of Nef (25μM) (Figure 2A and B). These results indicate that Nef strongly inhibits the anchorage-independent growth of both HeLa and SiHa cells. Figure 2C, shows that quantitative analysis of aggregated colonies of both cervical cancer cells against different concentrations of Nef (10, 25 and 50 μM) which indicated that there is a significant difference between controls and treatments ($P < 0.01$). In addition, Nef inhibits the clonogenic ability of cervical cancer cells in the colony formation assay (Figure 2D and 2E). In this assay, robust inhibition of colonies was observed in 25 and 50μM of Nef compared to control cervical cancer cell lines. We further examined the migration inhibitory effect of Nef

on HeLa and SiHa cells by using Transwell migration assays. The result of this assay showed that Nef dose-dependently inhibited the cell migration of both HeLa and SiHa cervical cancer cells to the bottom side of the insert and the bottom chamber (Figure 3A and C). The quantification of number of migrated cells in bottom of insert and chamber is presented in Figure 3B & D.

3.2 Nef induces oxidative stress through the production of reactive oxygen species (ROS), induces apoptosis and cell cycle arrest

Generation of endogenous reactive oxygen species was measured by confocal immunofluorescence microscope using DCFDA (2',7' -dichlorofluorescin diacetate) probe. Our data revealed that Nef induces oxidative stress through ROS production in a dose dependant manner significantly from 10μM onwards, indicated by the presence of strong green fluorescent color compared to control cells (Figure 4A). The antioxidant N-acetyl cysteine (NAC) abrogated the ROS producing effect of Nef. ROS production in terms of DCFDA fluorescent intensity induced by Nef was quantified by image-J software (Supplementary Figure 3). Apoptosis is an effective mechanism for the induction of cell death in cancer cells. To investigate the effect of Nef on apoptosis induction by fluorescence confocal imaging, both HeLa and SiHa cells were treated with different concentrations (10, 25 and 50μM) of Nef for 48hrs. Nef-treated cells were stained with Annexin V-FITC and PI to detect apoptosis, as shown in Figure 4B. Nef triggered significant nuclear condensation in cervical cancer cells, indicating apoptosis. These results confirmed that Nef induced apoptosis in HeLa and SiHa cells. To further investigate the cell cycle inhibitory potential effect of Nef on HeLa and SiHa cells, a cell cycle analysis was performed by flow cytometry using propidium iodide (PI). Cell cycle distribution analysis as shown in Figure 4C, which indicated that dose dependent G0/G1-phase arrest enforced by Nef in these cells. This result strongly suggests that Nef inhibited cell proliferation by inducing cell cycle arrest in the G0/G1 phase.

3.3 Nef induces apoptosis through DNA damage response

Morphological alterations in HeLa and SiHa cells after treatment with Nef were qualitatively investigated using fluorescent dye DAPI based on nuclear staining. Chromatin condensation, shrinking of the cells, nuclear margination, and apoptotic bodies appeared after exposure to 25μM Nef (Figure 5A). Furthermore, our confocal immunofluorescence analysis data showed that Nef treatment (25 μM) activated the expression of DNA damage response marker (pH_2AX) and apoptosis specific marker expression (cytochrome c) in HeLa and SiHa cells (Figure 5B and 5C).

3.4 Nef induced apoptosis studied by western blot analysis.

Further, to evaluate the Nef induced apoptosis signalling molecules in cervical cancer (HeLa and SiHa) cells by western blot analysis (Figure 6A), we determined the status of intrinsic apoptotic markers such as bcl-2, bax, cytochrome c, caspase-3, 9, procaspase-3 and 9, TCTP and PARP1. Our results showed that pro-apoptotic markers such as cytochrome c, Bax, cleaved caspase-3, 9 and cleaved PARP1 were up regulated, whereas, Bcl-2, TCTP, procaspase-3 and −9 were significantly down regulated in a dose dependent manner. Additionally, we have also validated the expression of Bcl-2 and Bax by real time-PCR

(Figure 6C), the data of which also shown increased mRNA expression of bax and reduction of bcl-2. These data strongly demonstrate that Nef induced mitochondrial mediated apoptosis in HeLa and SiHa cells (Figure 6A).

3.5 Nef induces autophagy by the activation of LC-3 by immunofluorescence

Over the past few decades, anti-cancer drug development has been based on the induction of apoptosis. However, cancer cells trigger multiple pathways in order to restore cancer cells from apoptosis (Pentimalli et al., 2018). Autophagy, a dynamic intracellular recycling process which eliminates accumulation of damaged proteins or organelles via transport to the lysosomes for degradation (Yuan et al., 2018). Therefore, activation of apoptosis and autophagy could effectively eliminate cancer cells. In addition to apoptosis induction, the anti-proliferative effects of Nef were also abrogated in the presence of autophagy inhibitor 3 methyladenine (3-MA) suggesting that autophagy may have a role in the anticancer effects of Nef. As the conversion of LC3 protein from LC3-I to LC3-II correlate with the extent of autophagy, we analyzed the conversion of cytosolic LC3-I into LC3-II through immunofluorescence. As presented in Figure 7A, Nef treated cells have more LC3 punctate dots than the control cells in both HeLa and SiHa cells. To further confirm, whether LC3 was involved in Nef-induced autophagy, the pEGFP-LC3 plasmid was transiently transfected into both HeLa and SiHa cells. As shown in Figure 7B, the control cells revealed diffused and weak LC3 punctate dots, whereas the Nef treated cells exhibited sharp green LC3 punctate dots in the cytoplasm, which indicates the accumulation of LC3-II in Nef treated HeLa and SiHa cells. The accumulation was more pronounced with the increasing dose of Nef.

3.6 Nef induced autophagic vacuoles detected by monodansylcadaverine (MDC) stain

Confocal microscopic analysis was used to identify the formation of autophagic vacuoles during autophagy. The fluorescent dye MDC is a specific marker for autophagy that could specifically stain autophagosomes to detect the occurrence of autophagic vacuoles. Nef induces autophagy by lysophagosome formation, as shown in Figure 7C, the number of MDC-labeled vesicles within HeLa and SiHa cervical cells was significantly increased with Nef treatment as compared to control, confirming that Nef induces accumulation of autophagic vacuoles. The autophagy inhibitor 3-MA is commonly used to define the role of autophagy under various physiological conditions (Shan et al., 2017). To elucidate the role of autophagy in the HeLa and SiHa cells treated with Nef, we used autophagy inhibitors 3MA (which blocks the fusion of autophagosomes and lysosomes). Pretreatment with 3-MA (2.5mM) effectively decreases the activation of Nef-induced MDC incorporation (Figure 7C) in cells treated with Nef plus 3-MA. Activation of autophagic vacuole formation was further confirmed using LysoTracker, green fluorescent dye that stains lysosomes. As shown in Supplementary Figure 4, the fluorescence of Lysotracker green increased after treatment with Nef (25 μM).

3.7 Western blot analysis of autophagy related proteins

Additionally, Nef induced autophagy related proteins were determined by western blot analysis as shown in Figure 8A. The results revealed that Nef treatment induced processing of full-length LC3-I to LC3-II conversion, indicating an increased formation of

autophagosomes induced by Nef. Beclin1, atg-4, −5 and −12 are the key determining factors in the initiation of autophagy, which is involved in the formation of autophagosomes. Data revealed that up regulated expression of beclin-1, atg-4,−5, and −12 proteins in HeLa and SiHa cells. expression, Interestingly, p62/ SQSTM1 was significantly increased following Nef treatment in a dose dependent manner, the up regulation indicates autophagy induction as p62/ SQSTM1 is a marker protein involved in the degradation of autophagosomes. Atg-4 is a redox regulated cysteine protease, which is considered to play an essential role in the ROS-mediated autophagy (Lv et al., 2017). Our result showed that Atg-4 was elevated with increasing doses of treatment suggesting that Nef induced ROS mediated autophagy in Hela and SiHa cells involving induction of atg4 protein.

3.8 Neferine downregulates HPV early genes (HPV E6 and E7) and modulates autophagy/ apoptosis markers

Nef induced autophagy was further confirmed by the validation of key autophagy regulated genes (Beclin-1 and LC3) at mRNA level using RT-PCR. Quantitative analysis of mRNA, demonstrated that cancer cells treated with Nef markedly upregulated beclin-1 (initiation factor for autophagosome formation) and promoted the expression of LC3 as compared to the control (Figure 8C). Importantly, HPV early genes (E6 and E7) were also downregulated in Nef treated cells compared to controls.

Taken together, these multifactorial anti-cancer effects of Nef appear to inhibit the malignant properties of cervical cancer cells through inducing both apoptosis and autophagy process as shown in Figure 9.

4. DISCUSSION

Treatment rates of recent chemotherapy is far from desirable and requires formulating strategies to enhance the specificity and efficacy of available anticancer regimes. Cervical cancer is one of the most common solid tumors and remains to be one of the leading causes of cancer-related deaths in women. Therefore, there is a crucial need for the development of strategies that could effectively treat cervical cancer with less side effects. It has been reported Nef regulated apoptosis and autophagy cell death involving ROS in osteosarcoma, liver and lung cancer (Poornima et al., 2013b, 2014; Zhang et al., 2012). However, the molecular mechanisms for Nef induced ROS mediated apoptosis remains unclear and whether the role of atg4 in autophagy induced cell death in cervical cancer cells is yet to be demonstrated. Considering these notions, we studied the effect of Nef on cervical cancer cells (HeLa and SiHa cells) using *in vitro* models. Our data revealed that Nef displayed robust anticancer effects in both HeLa and SiHa cervical cancer cells (Figure 1A) while showing minimal toxic effects to HEK-293 cells (Figure 1D). In comparison to other reported anti-cervical cancer natural compounds (Table 1), Nef appears to be a potent anticancer agent for cervical cancer.

The major strategies of anticancer drugs include inhibition of cell proliferation or inducing apoptosis in cancer cells. In the present study, Nef inhibited the *in vitro* growth of cervical cancer cells (Hela and SiHa cells) in dose dependent manner. As shown in figure 1A, Nef inhibits the growth of HeLa and SiHa cells at a concentration of 25 μM at 48 hrs. However,

HeLa cells were more sensitive than the SiHa cells. The present results are consistent with previous results supporting that Nef inhibits the growth of cancer cells including lung and hepatocellular carcinoma (HCC) (Poornima et al., 2013a). Since Nef is a natural dietary constituent, toxicity associated with Nef for normal cells is expected to be very low as we have shown in HEK-293 cells. Anti-proliferative effects of Nef was significantly abrogated by anti-oxidant N-acetyl cysteine (NAC) and autophagy inhibitor 3-Methyladenine (3-MA) and partially abrogated by the caspase inhibitor (Z-VAD-FMK) suggesting that ROS mediated autophagy and apoptosis are the underlying anti-cancer mechanism of Nef in HeLa and SiHa cells. Soft agar colony formation assay is a well-established method to evaluate cellular anchorage-independent growth for the detection of the tumorigenic potential of malignant cells (Yuan et al., 2017). Nef also inhibited anchorage independent growth of cervical cancer cells in HeLa and SiHa cells when compared to untreated control cells. We evaluated the effect of Nef on the growth of HeLa and SiHa cells and their capacity to form colonies in a soft-agar and colony formation assay, in which we have observed inhibition of colony formation in Nef treatment. In addition to suppression of anchorage independent growth, robust inhibition in colony formation was observed in cervical cancer cell lines (HeLa and SiHa) at 25 and 50 μM concentrations compared to control cells, which is in correlation with the inhibitory effect of Nef on hepatocellular carcinoma (Deng et al., 2017).

The involvement of ROS in the execution of cell death is a well-known phenomenon. ROS are important signaling molecules in various cellular processes such as growth, differentiation, and apoptosis (Velavan et al., 2018). Most cancer cells undergo oxidative stress due to the increased production of intrinsic ROS (Poornima et al., 2013b). For instance, ROS can also function as a molecular signal to mediate the initiation of autophagy, apoptosis and at times both (Kalai Selvi et al., 2017; Pelicano et al., 2004). In fact, several anticancer agents were shown to arbitrate their effect through the induction of ROS, and inhibition of ROS production by antioxidants block autophagy and cell death in many cancer types (Al Dhaheri et al., 2014; Karna et al., 2010; Rikiishi, 2012; Shrivastava et al., 2011). Recent studies showed that the production of ROS, in response to anticancer agents, elicits different responses in cancer cells. While low level of ROS was shown to induce autophagy, excessive ROS accumulation triggered both apoptosis and autophagy (Zhang et al., 2015). Therefore, the role of ROS in Nef induced cell death was investigated. Nef treatment increased the intensity of DCF fluorescence in both HeLa and SiHa cells, implicating that intracellular ROS was increased. We found that, the treatment of HeLa and SiHa cells with different concentrations of Nef resulted in a dose dependent increase in ROS. A prolonged exposure of Nef led to the excessive ROS production, which ultimately resulted in higher levels of oxidative damage that exceeds the cell’s repair capabilities that eventually caused programmed cell death through activation of intrinsic and extrinsic apoptotic pathways. Abrogation of ROS production by the ROS scavenger NAC, totally blocked the anticancer effect of Nef suggesting that Nef mediates its anticancer effects via ROS generation. ROS were also found to regulate caspase-dependent apoptosis, through the activation of a series of caspases (caspase-8, caspase-9, and eventually caspase-3) activation. In the present study, Nef induced ROS activates the release of cytochrome C and followed by caspase 3 & 9 mediated apoptosis. Our western blot analysis showed that increasing the expression of pro-apoptotic proteins bax, cytochrome-C, cleaved caspase-3 and 9 and PARP1 cleavage

indicating apoptosis activation respectively following Nef treatment in cervical cancer cells. On the other hand, Nef downregulated the expression of bcl-2, caspase-3 & 9 and TCTP in cervical cancer cells. TCTP is an important anti-apoptotic marker, which plays key roles in cell proliferation and anti-apoptosis through interaction with MCL1 and Bax. TCTP also acts as a transcription factor in the regulation of stem cell genes Oct4 and Nanog (Chen et al., 2014). Thus, Nef effectively targets cervical cancer cells by activating apoptosis while suppressing TCTP expression. The cell cycle progression is a hallmark of tumorigenesis. Our results infer that Nef led to a G0/G1 phase arrest. Together, our results suggest that ROS might have a major role in inducing apoptosis and cell cycle arrest in Nef treated HeLa and SiHa cells.

Autophagy is a well-conserved lysosomal degradation pathway that has become an attractive and alternative therapeutic approach for targeting cancer using chemotherapeutic drugs (Levine, 2007). ROS have been reported to be involved in autophagy by regulating the activity of the redox sensitive cysteine protease HsAtg4A, which belongs to the Atg4 family (Scherz-Shouval et al., 2007). The thiol reduced form of Atg4 enables the conversion of LC3-I into LC3-II, lipidation and insertion into the autophagosome, and then recycles LC3-II after the autophagosome fuses with the lysosome (Lee et al., 2012). Here, to confirm Nef induced ROS mediated autophagy, by western blot analysis we determined the expression of atg protein complex that are involved in the initiation stages of autophagy markers such as beclin 1 which is required for formation of pre-autophagosome. Atg-5–12 complex are essential components of the autophagosome membrane while LC3I/II is required for elongation of autophagosomal membrane. The results (Figure 8A) demonstrate that the relative expression of beclin 1, atg −5, −12, conversion of LC3I/LC3II as well as adaptor protein P62/SQSTM1 were significantly up regulated in a dose dependent manner suggesting that Nef is involved in both initiation and elongation steps of autophagy. Further, our data showed that Nef dose dependently increased atg4 expression implicating that ROS mediated autophagy occurring in HeLa and SiHa cells. These results also correlated with increased mRNA expression of beclin 1 and LC3 contributing to autophagy (Figure 8C). Our findings support that Nef is a dual inducer of both apoptosis and autophagy activation in cervical cancer cells. Then we proceeded to investigate the expression level of HPV early genes, E6 and E7 after Nef treatment. Data from PCR analysis showed that Nef in both cervical cancer cells significantly suppressed the expressions of HPV E6 and HPV E7 (Figure 8B and C). Similarly, Mahata et al. also reported that a naturally occurring isoquinoline alkaloid, berberine, selectively suppress expression of HPV16E6, HPV16E7, HPV18E6 and HPV18E7 through transcription factor AP-1 in a dose and time dependent manner (Mahata et al., 2011). Therefore, our results confirm the Nef induced ROS triggered autophagy in HeLa and SiHa cells.

In summary, we have demonstrated a potential role of ROS in the initiation of mitochondrial dependent apoptosis as well as role of atg4 in autophagy by Nef-treated cervical cancer cells. Our results provide new insight into the anticancer effect of Nef via ROS signaling in mediating both apoptosis and autophagy in synergistic targeting cervical cancer cells. As Nef induced mitochondrial mediated cell death through cytochrome c and bax, we believe that Nef induces ROS generation in mitochondria which needs further confirmation. Also, whether atg4 as Nef target need to be further confirmed in live models. Future *in vivo*

studies and characterizing additional signaling pathways targeted by Nef will help develop this natural compound as a potential treatment for cervical cancer.

Supplementary Material

Refer to Web version on PubMed Central for supplementary material.

ACKNOWLEDGEMENTS

This study was partly supported by funding received from NIH, United States (R03 CA212890-01A1, R03 CA227218, and R03 CA230829) and UIC-NIH Botanical Center Pilot Grant award (parent grant P50 AT 000155).

Abbreviations:

Nef	Neferine
ROS	Reactive oxygen species
HPV	human papillomavirus
MDC	monodansylcadaverine
LC3	light chain 3

References

Al Dhaheri Y, Attoub S, Ramadan G, Arafat K, Bajbouj K, Karuvantevida N, AbuQamar S, Eid A, Iratni R, 2014 Carnosol induces ROS-mediated beclin1-independent autophagy and apoptosis in triple negative breast cancer. PloS one 9, e109630. [PubMed: 25299698]

Asokan SM, Mariappan R, Muthusamy S, Velmurugan BK, 2018 Pharmacological benefits of neferine-A comprehensive review. Life sciences, 199, pp.60–70. [PubMed: 29499283]

Bai C, Yang X, Zou K, He H, Wang J, Qin H, Yu X, Liu C, Zheng J, Cheng F and Chen J, 2016 Anti-proliferative effect of RCE-4 from Reineckia carnea on human cervical cancer HeLa cells by inhibiting the PI3K/Akt/mTOR signaling pathway and NF-κB activation. Naunyn-Schmiedeberg's archives of pharmacology, 389(6), 573–584.

Baskaran R, Poornima P, Huang CY and Padma VV, 2016 Neferine prevents NF-κB translocation and protects muscle cells from oxidative stress and apoptosis induced by hypoxia. Biofactors, 42(4), 407–417. [PubMed: 27041079]

Bray F, Ferlay J, Soerjomataram I, Siegel RL, Torre LA, Jemal A, 2018 Global cancer statistics 2018: GLOBOCAN estimates of incidence and mortality worldwide for 36 cancers in 185 countries. CA: a cancer journal for clinicians 68, 394–424. [PubMed: 30207593]

Cao W, Li XQ, Wang X, Fan HT, Zhang XN, Hou Y, Liu SB and Mei QB, 2010 A novel polysaccharide, isolated from Angelica sinensis (Oliv.) Diels induces the apoptosis of cervical cancer HeLa cells through an intrinsic apoptotic pathway. Phytomedicine, 17(8–9), 598–605. [PubMed: 20092988]

Chen K, Huang C, Yuan J, Cheng H, Zhou R, 2014 Long-term artificial selection reveals a role of TCTP in autophagy in mammalian cells. Mol Biol Evol 31, 2194–2211. [PubMed: 24890374]

Chinnapaka S, Zheng G, Chen A and Munirathinam G, 2019 Nitro aspirin (NCX4040) induces apoptosis in PC3 metastatic prostate cancer cells via hydrogen peroxide (H2O2)-mediated oxidative stress. Free Radical Biology and Medicine, 143, 494–509. [PubMed: 31446057]

Dasari S, Samy A, Kajdacsy-Balla A, Bosland MC, Munirathinam G, 2018a Vitamin K2, a menaquinone present in dairy products targets castration-resistant prostate cancer cell-line by activating apoptosis signaling. Food and chemical toxicology : an international journal published for the British Industrial Biological Research Association 115, 218–227. [PubMed: 29432837]

Dasari S, Samy A, Narvekar P, Dontaraju VS, Dasari R, Kornienko A, Munirathinam G, 2018b Polygodial analog induces apoptosis in LNCaP prostate cancer cells. European journal of pharmacology 828, 154–162. [PubMed: 29572068]

Deng G, Zeng S, Ma J, Zhang Y, Qu Y, Han Y, Yin L, Cai C, Guo C, Shen H, 2017 The anti-tumor activities of Neferine on cell invasion and oxaliplatin sensitivity regulated by EMT via Snail signaling in hepatocellular carcinoma. Scientific reports 7, 41616. [PubMed: 28134289]

Eid W, Abdel-Rehim W, 2017 Neferine Enhances the Antitumor Effect of Mitomycin-C in Hela Cells Through the Activation of p38-MAPK Pathway. Journal of cellular biochemistry 118, 3472–3479. [PubMed: 28328092]

Farooqui A, Khan F, Khan I, & Ansari IA 2018 Glycyrrhizin induces reactive oxygen species-dependent apoptosis and cell cycle arrest at G0/G1 in HPV18+ human cervical cancer HeLa cell line. Biomedicine & Pharmacotherapy, 97, 752–764. [PubMed: 29107932]

Ghasemi F, Shafiee M, Banikazemi Z, Pourhanifeh MH, Khanbabaei H, Shamshirian A, Moghadam SA, ArefNezhad R, Sahebkar A, Avan A and Mirzaei H, 2019 Curcumin inhibits NF-kB and Wnt/β-catenin pathways in cervical cancer cells. Pathology-Research and Practice, 215(10), 152556.

Guan G, Han H, Yang Y, Jin Y, Wang X and Liu X, 2014 Neferine prevented hyperglycemia-induced endothelial cell apoptosis through suppressing ROS/Akt/NF-κB signal. Endocrine, 47(3), 764–771. [PubMed: 24590293]

Hu YL, Jahangiri A, Delay M, Aghi MK, 2012 Tumor cell autophagy as an adaptive response mediating resistance to treatments such as antiangiogenic therapy. Cancer research 72, 4294–4299. [PubMed: 22915758]

Kalai Selvi S, Vinoth A, Varadharajan T, Weng CF, Vijaya Padma V, 2017 Neferine augments therapeutic efficacy of cisplatin through ROS- mediated non-canonical autophagy in human lung adenocarcinoma (A549 cells). Food and chemical toxicology : an international journal published for the British Industrial Biological Research Association 103, 28–40. [PubMed: 28223119]

Karna P, Zughaier S, Pannu V, Simmons R, Narayan S, Aneja R, 2010 Induction of reactive oxygen species-mediated autophagy by a novel microtubule-modulating agent. The Journal of biological chemistry 285, 18737–18748. [PubMed: 20404319]

Kadioglu O, Law BY, Mok SW, Xu SW, Efferth T and Wong VK, 2017 Mode of action analyses of neferine, a bisbenzylisoquinoline alkaloid of lotus (Nelumbo nucifera) against multidrug-resistant tumor cells. Frontiers in pharmacology, 8, 238. [PubMed: 28529482]

Kedhari Sundaram M, Raina R, Afroze N, Bajbouj K, Hamad M, Haque S Hussain A, 2019 Quercetin modulates signaling pathways and induces apoptosis in cervical cancer cells. Bioscience reports, 39(8).

Kuo CY, Schelz Z, Tóth B, Vasas A, Ocsovszki I, Chang FR, Hohmann J, Zupkó I Wang HC, 2019 Investigation of natural phenanthrenes and the antiproliferative potential of juncusol in cervical cancer cell lines. Phytomedicine, 58, 152770. [PubMed: 31005716]

Lee J, Giordano S, Zhang J, 2012 Autophagy, mitochondria and oxidative stress: cross-talk and redox signalling. The Biochemical journal 441, 523–540. [PubMed: 22187934]

Levine B, 2007 Cell biology: autophagy and cancer. Nature 446, 745–747. [PubMed: 17429391]

Li H, Wu X, 2016 Advances in diagnosis and treatment of metastatic cervical cancer. 27, e43.

Li M, He Y, Peng C, Xie X and Hu G, 2018 Erianin inhibits human cervical cancer cell through regulation of tumor protein p53 via the extracellular signal-regulated kinase signaling pathway. Oncology letters, 16(4), 5006–5012. [PubMed: 30250566]

Li W, Li S, Li Y, Lin X, Hu Y, Meng T, Wu B, He R and Feng D, 2018 Immunofluorescence staining protocols for major autophagy proteins including LC3, P62, and ULK1 in mammalian cells in response to normoxia and hypoxia In Autophagy in Differentiation and Tissue Maintenance 175–185. Humana Press, New York, NY.

Li XC, Tong GX, Zhang Y, Liu SX, Jin QH, Chen HH, Chen P, 2010 Neferine inhibits angiotensin II-stimulated proliferation in vascular smooth muscle cells through heme oxygenase-1. Acta Pharmacol Sin 31, 679–686. [PubMed: 20523338]

Li ZY, Yang Y, Ming M and Liu B, 2011 Mitochondrial ROS generation for regulation of autophagic pathways in cancer. Biochemical and biophysical research communications, 414(1), 5–8. [PubMed: 21951851]

Liu F, Liu D, Yang Y, Zhao S, 2013 Effect of autophagy inhibition on chemotherapy-induced apoptosis in A549 lung cancer cells. Oncology letters 5, 1261–1265. [PubMed: 23599776]

Liu S, Wang B, Li XZ, Qi LF and Liang YZ, 2009 Preparative separation and purification of liensinine, isoliensinine and neferine from seed embryo of Nelumbo nucifera GAERTN using high-speed counter-current chromatography. Journal of separation science, 32(14), pp.2476–2481. [PubMed: 19557808]

Lv W, Sui L, Yan X, Xie H, Jiang L, Geng C, Li Q, Yao X, Kong Y and Cao J, 2018 ROS-dependent Atg4 upregulation mediated autophagy plays an important role in Cd-induced proliferation and invasion in A549 cells. Chemico-biological interactions, 279, 136–144. [PubMed: 29179951]

Mahata S, Bharti AC, Shukla S, Tyagi A, Husain SA, Das BC, 2011 Berberine modulates AP-1 activity to suppress HPV transcription and downstream signaling to induce growth arrest and apoptosis in cervical cancer cells. Molecular cancer 10, 39-39. [PubMed: 21496227]

Manogaran P, Beeraka NM and Padma VV, 2019 The Cytoprotective and Anti-cancer Potential of Bisbenzylisoquinoline Alkaloids from *Nelumbo nucifera*. Current topics in medicinal chemistry.

Newman DJ, Cragg GM, 2016 Natural Products as Sources of New Drugs from 1981 to 2014. Journal of natural products 79, 629–661. [PubMed: 26852623]

Nunez R, 2001 DNA measurement and cell cycle analysis by flow cytometry. Curr Issues Mol Biol 3, 67–70. [PubMed: 11488413]

Pan Y, Ke H, Yan Z, Geng Y, Asner N, Palani S, Munirathinam G, Dasari S, Nitiss KC, Bliss S and Patel P, 2016 The western-type diet induces anti-HMGB1 autoimmunity in Apoe−/− mice. Atherosclerosis, 251, 31–38. [PubMed: 27240253]

Paudel KR, Panth N, 2015 Phytochemical Profile and Biological Activity of *Nelumbo nucifer*a. Evidence-based complementary and alternative medicine : eCAM 2015, 789124. [PubMed: 27057194]

Pelicano H, Carney D, Huang P, 2004 ROS stress in cancer cells and therapeutic implications. Drug resistance updates : reviews and commentaries in antimicrobial and anticancer chemotherapy 7, 97–110. [PubMed: 15158766]

Peralta-Zaragoza O, Bermudez-Morales VH, Perez-Plasencia C, Salazar-Leon J, Gomez-Ceron C, Madrid-Marina V, 2012 Targeted treatments for cervical cancer: a review. OncoTargets and therapy 5, 315–328. [PubMed: 23144564]

Pentimalli F, Grelli S, Di Daniele N, Melino G and Amelio I, 2019 Cell death pathologies: targeting death pathways and the immune system for cancer therapy. Genes & Immunity, 20(7), 539–554. [PubMed: 30563970]

Pham DC, Chang YC, Lin SR, Fuh YM, Tsai MJ and Weng CF, 2018 FAK and S6K1 inhibitor, Neferine, dually induces autophagy and apoptosis in human neuroblastoma cells. Molecules, 23(12), 3110.

Poornima P, Quency RS, Padma VV, 2013a Neferine induces reactive oxygen species mediated intrinsic pathway of apoptosis in HepG2 cells. Food chemistry 136, 659–667. [PubMed: 23122111]

Poornima P, Weng CF, Padma VV, 2013b Neferine from *Nelumbo nucifera* induces autophagy through the inhibition of PI3K/Akt/mTOR pathway and ROS hyper generation in A549 cells. Food chemistry 141, 3598–3605. [PubMed: 23993526]

Poornima P, Weng CF, Padma VV, 2014 Neferine, an alkaloid from lotus seed embryo, inhibits human lung cancer cell growth by MAPK activation and cell cycle arrest. BioFactors (Oxford, England) 40, 121–131.

Rikiishi H, 2012 Novel Insights into the Interplay between Apoptosis and Autophagy. International journal of cell biology 2012, 317645. [PubMed: 22496691]

Scherz-Shouval R, Shvets E, Fass E, Shorer H, Gil L, Elazar Z, 2007 Reactive oxygen species are essential for autophagy and specifically regulate the activity of Atg4. The EMBO journal 26, 1749–1760. [PubMed: 17347651]

Seglen PO, Gordon PB, 1982 3-Methyladenine: specific inhibitor of autophagic/lysosomal protein degradation in isolated rat hepatocytes. Proceedings of the National Academy of Sciences of the United States of America 79, 1889–1892. [PubMed: 6952238]

Shao FY, Wang S, Li HY, Chen WB, Wang GC, Ma DL, Wong NS, Xiao H, Liu QY, Zhou GX and Li YL, 2016 EM23, a natural sesquiterpene lactone, targets thioredoxin reductase to activate JNK and cell death pathways in human cervical cancer cells. Oncotarget, 7(6), 6790. [PubMed: 26758418]

Shetty A, Dasari S, Banerjee S, Gheewala T, Zheng G, Chen A, Kajdacsy-Balla A, Bosland MC and Munirathinam G, 2016, 11 Hepatoma-derived growth factor: A survival-related protein in prostate oncogenesis and a potential target for vitamin K2. In Urologic Oncology: Seminars and Original Investigations Vol. 34, No. 11, 483–e1.

Shrivastava A, Kuzontkoski PM, Groopman JE, Prasad A, 2011 Cannabidiol induces programmed cell death in breast cancer cells by coordinating the cross-talk between apoptosis and autophagy. Molecular cancer therapeutics 10, 1161–1172. [PubMed: 21566064]

Siegel RL, Miller KD, & Jemal A 2020 Cancer statistics, 2020. CA: A Cancer Journal for Clinicians, 70(1), 7–30. [PubMed: 31912902]

Singh S, Sharma B, Kanwar SS, Kumar A, 2016 Lead Phytochemicals for Anticancer Drug Development. Front Plant Sci 7, 1667. [PubMed: 27877185]

Tang YS, Zhao YH, Zhong Y, Li XZ, Pu JX, Luo YC and Zhou QL, 2019 Neferine inhibits LPS-ATP-induced endothelial cell pyroptosis via regulation of ROS/NLRP3/Caspase-1 signaling pathway. Inflammation Research, 68(9), 727–738. [PubMed: 31172209]

Trybus W, Krol T, Trybus E, Stachurska A, Krol G and Kopacz-Bednarska A, 2019 Emodin Induces Death in Human Cervical Cancer Cells Through Mitotic Catastrophe. Anticancer research, 39(2), 679–686. [PubMed: 30711945]

Velavan B, Divya T, Sureshkumar A and Sudhandiran G, 2018 Nano-chemotherapeutic efficacy of (−)-epigallocatechin 3-gallate mediating apoptosis in A549 cells: Involvement of reactive oxygen species mediated Nrf2/Keap1signaling. Biochemical and biophysical research communications, 503(3), 1723–1731. [PubMed: 30075845]

Wang KS, Lv Y, Wang Z, Ma J, Mi C, Li X, Xu GH, Piao LX, Zheng SZ and Jin X, 2017 Imperatorin efficiently blocks TNF-α-mediated activation of ROS/PI3K/Akt/NF-κB pathway. Oncology reports, 37(6), 3397–3404. [PubMed: 28440462]

Warowicka A, Łukasz P, Grażyna B, Oskar M, Jagoda LC, Dorota K, Robert N, Stefan J and Anna GJ, 2019 Protoberberine compounds extracted from Chelidonium majus L. as novel natural photosensitizers for cancer therapy. Phytomedicine, 64, 152919. [PubMed: 31465980]

Xie Z, Wei Y, Xu J, Lei J, & Yu J 2019 Alkaloids from Piper nigrum synergistically enhanced the effect of paclitaxel against paclitaxel-resistant cervical cancer cells through the downregulation of Mcl-1. Journal of agricultural and food chemistry, 67(18), 5159–5168. [PubMed: 31006247]

Xu L, Zhang X, Li Y, Lu S, Lu S, Li J, Wang Y, Tian X, Wei JJ, Shao C and Liu Z, 2016 Neferine induces autophagy of human ovarian cancer cells via p38 MAPK/JNK activation. Tumor Biology, 37(7), 8721–8729. [PubMed: 26738868]

Yang D, Zou X, Yi R, Liu W, Peng D and Zhao X, 2016 Neferine increase in vitro anticancer effect of dehydroepiandrosterone on MCF-7 human breast cancer cells. Applied Biological Chemistry, 59(4), 585–596.

Yang SY, Kim NH, Cho YS, Lee H, Kwon HJ, 2014 Convallatoxin, a dual inducer of autophagy and apoptosis, inhibits angiogenesis in vitro and in vivo. PloS one 9, e91094. [PubMed: 24663328]

Yuan P, He XH, Rong YF, Cao J, Li Y, Hu YP, Liu Y, Li D, Lou W, Liu MF, 2017 KRAS/NF-kappaB/YY1/miR-489 Signaling Axis Controls Pancreatic Cancer Metastasis. Cancer research 77, 100–111. [PubMed: 27793842]

Yuan X, Wang B, Yang L and Zhang Y, 2018 The role of ROS-induced autophagy in hepatocellular carcinoma. Clinics and research in hepatology and gastroenterology, 42(4), 306–312. [PubMed: 29544680]

Zaman MS, Chauhan N, Yallapu MM, Gara RK, Maher DM, Kumari S, Sikander M, Khan S, Zafar N, Jaggi M and Chauhan SC, 2016 Curcumin nanoformulation for cervical cancer treatment. Scientific reports, 6, 20051. [PubMed: 26837852]

Zhang L, Wang K, Lei Y, Li Q, Nice EC and Huang C, 2015 Redox signaling: Potential arbitrator of autophagy and apoptosis in therapeutic response. Free Radical Biology and Medicine, 89, 452–465. [PubMed: 26454086]

Zhang X, Liu Z, Xu B, Sun Z, Gong Y, Shao C, 2012 Neferine, an alkaloid ingredient in lotus seed embryo, inhibits proliferation of human osteosarcoma cells by promoting p38 MAPK-mediated p21 stabilization. European journal of pharmacology 677, 47–54. [PubMed: 22227330]

Zur Hausen H, 2008 Novel human polyomaviruses--re-emergence of a well known virus family as possible human carcinogens. International journal of cancer 123, 247–250. [PubMed: 18449881]

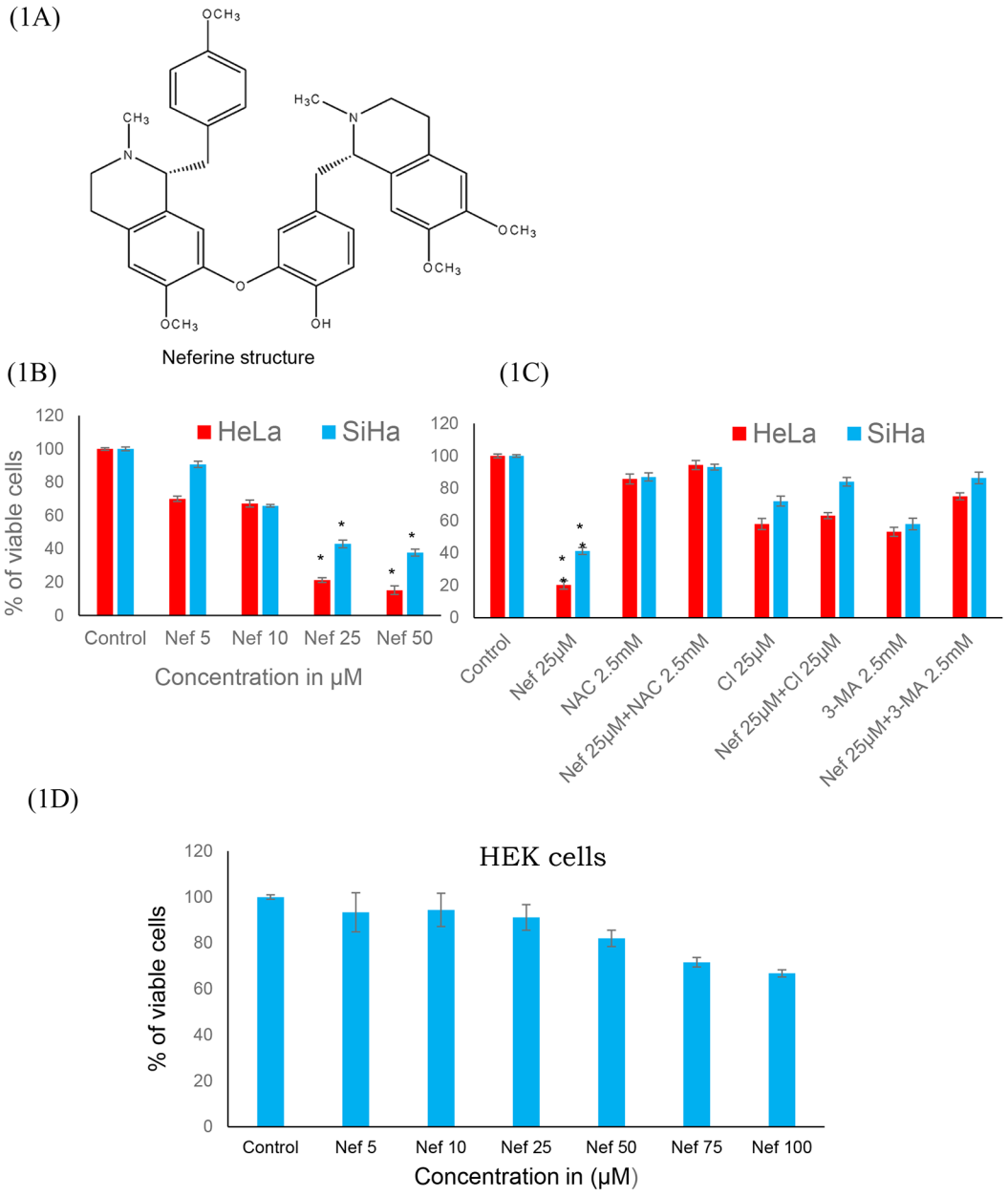

Figure 1: Nef inhibits the proliferation of cervical cancer cells:

(A) Chemical structure of the Neferine. **(B)** Nef inhibits the proliferation of cervical cancer cells (HeLa and SiHa cells) in a dose dependent manner (48 hrs) as determined by MTT cell proliferation assay. **(C)** 25μM concentration of Nef shows inhibitory concentration (IC_{50}) at 48hrs and the effects of Nef was abrogated by antioxidant (NAC), autophagy inhibitor (3MA) and caspase inhibitor (CI) (Z-VAD-FMK). **(D)** Cytotoxicity analysis of Nef on normal kidney cells HEK-293. Cells were treated with various concentrations of Nef (0 to 100μM), results indicate no significant cytotoxicity. Data shown as mean ± SD. *$p< 0.01$ for differences between controls and Nef treatments; $^{\#}p< 0.01$ for differences between Nef 25μM and Nef 25μM plus NAC inhibitor.

(2A) HeLa

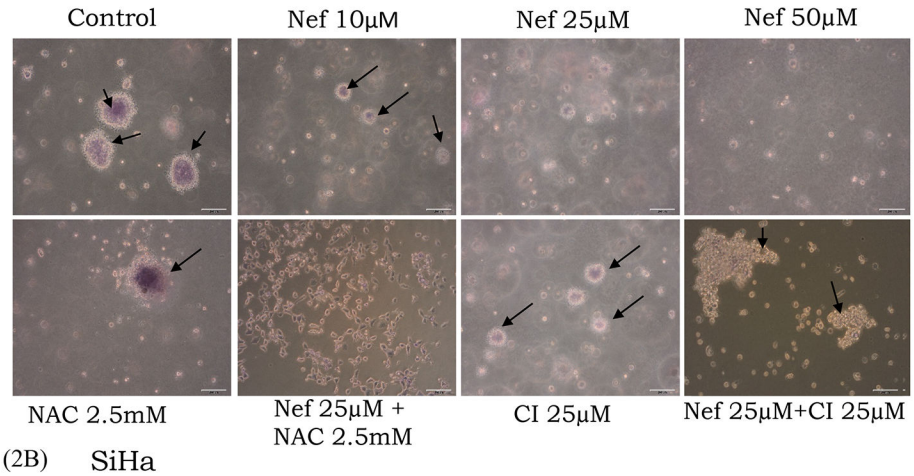

(2B) SiHa

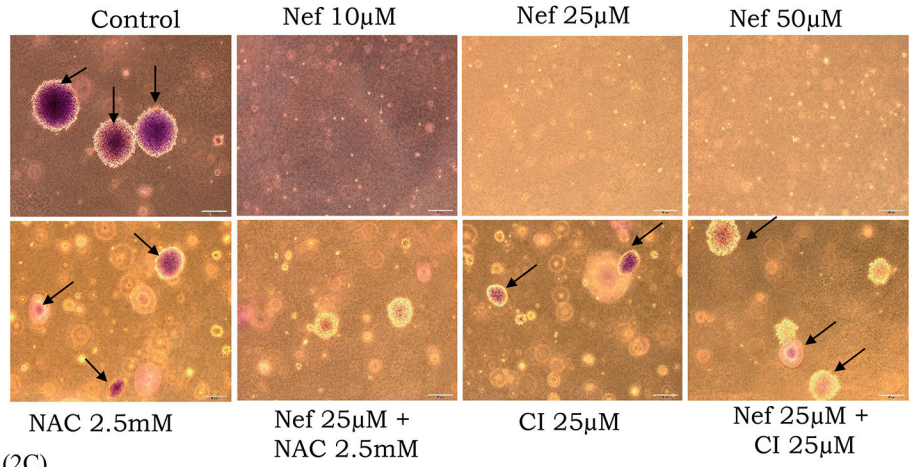

(2C)

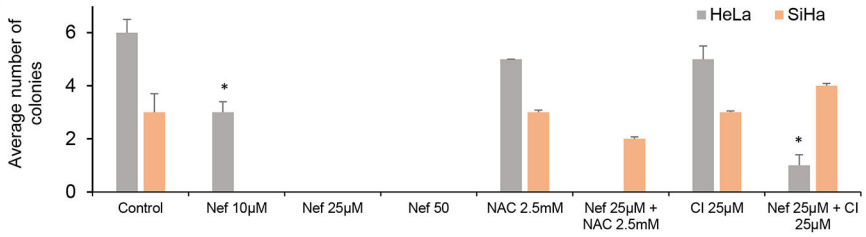

(2D)

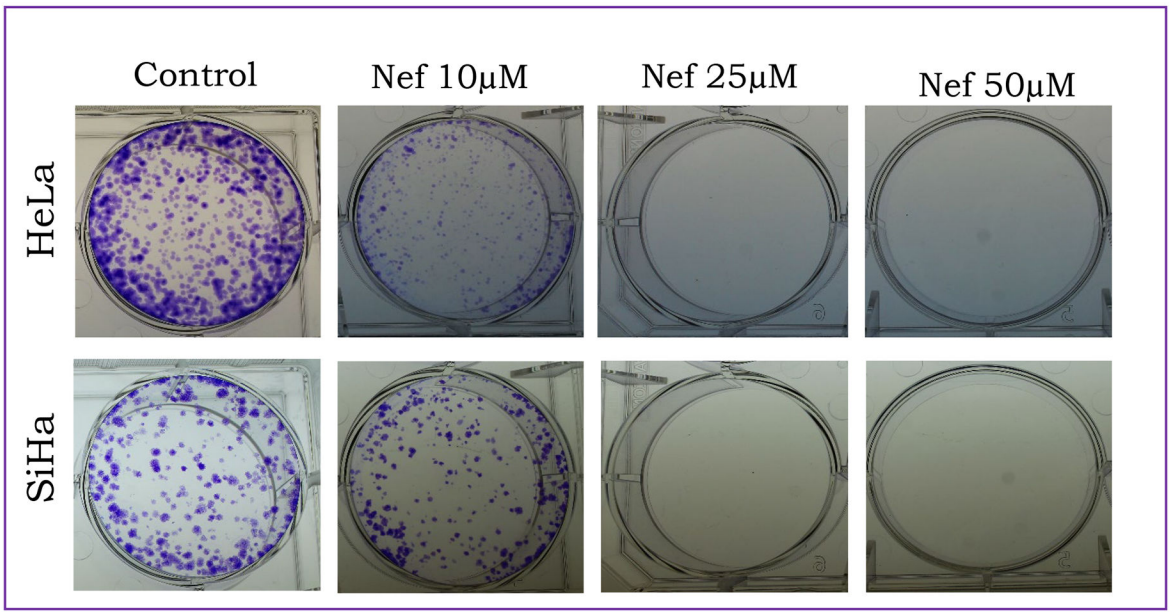

(2E)

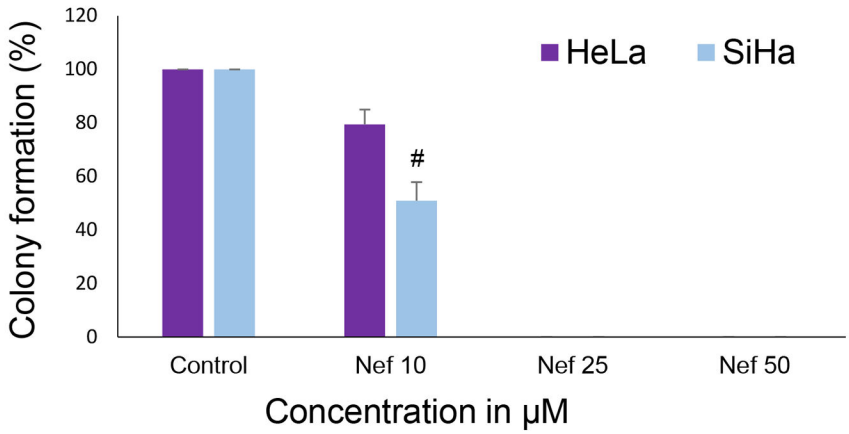

Figure 2: Nef treatment reduces anchorage-independent growth of cervical cancer cells: **(A** and **B)** Soft agar assay results showed that Nef significantly inhibit the colony formation ability of cervical cancer cells. Colonies were detected using crystal violet staining. **(C)** Colonies were counted and represented in a graph showing that the average number of colonies in the control cells versus Nef-treated cells. Arrow indicates stained colonies. *p<0.01 for difference between Nef treatments and controls. **Nef treatment induces inhibition of colony formation ability of cervical cancer cells: (D)** Clonogenic assay results showed that Nef suppresses the colony forming ability of cervical cancer cells. Colonies were detected using crystal violet staining. **(E)** Quantified results showing that Nef robustly inhibits the colony forming ability of both HeLa and SiHa cervical cancer cells. #p<0.01 for difference between Nef treatment and control.

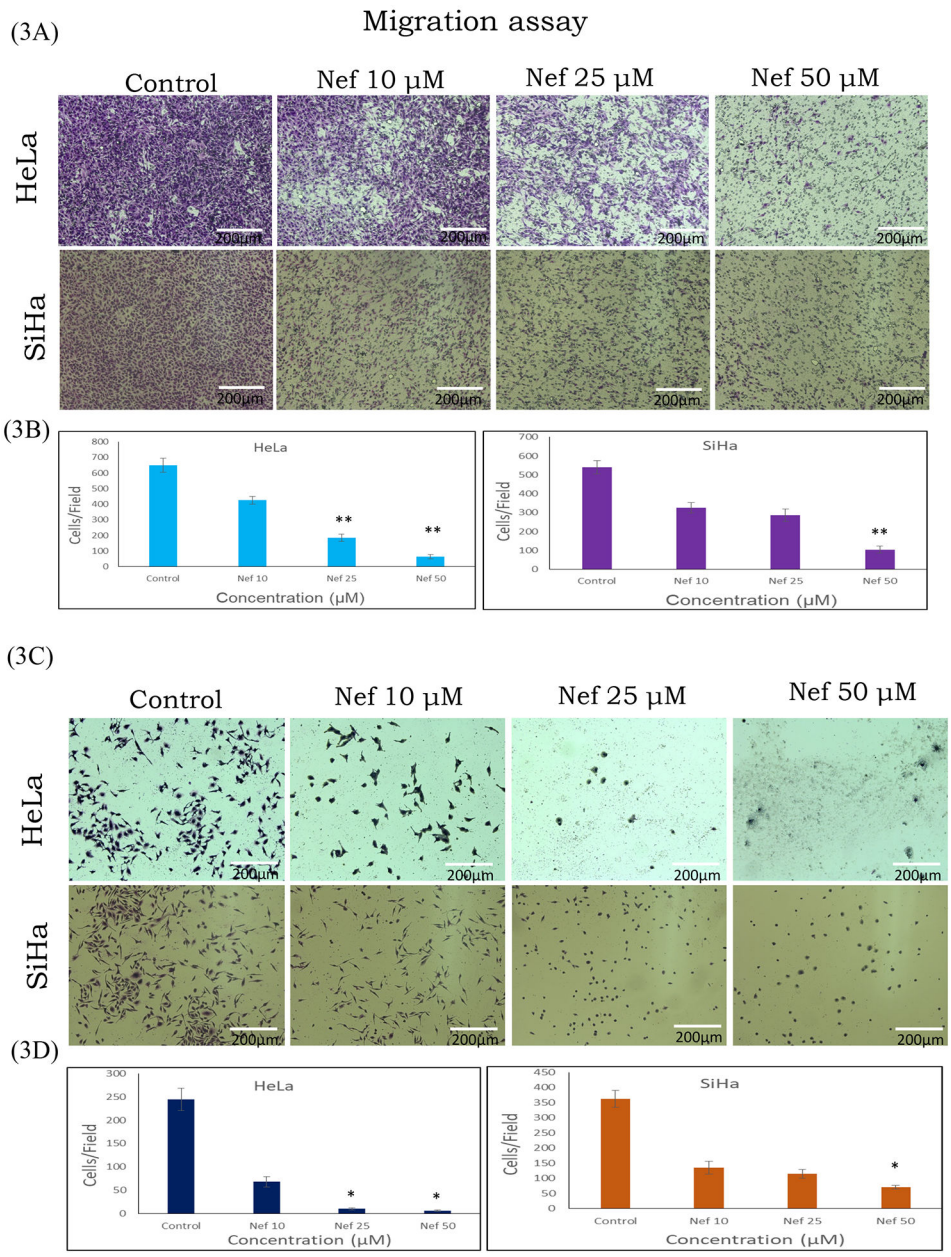

Figure 3: Transwell migration assay:

Inhibitory effect of Nef on the migration of HeLa and SiHa cells were determined by Transwell migration assay for 48hrs with different concentration of Nef (10, 25 and 50µM). Results showed that Nef significantly inhibit migration of HeLa and SiHa cells **(A)** Migrated cells to the bottom side of the Trasnwell membrane insert; **(C)** Migrated cells to the bottom well of the chamber. Figure **(B & D)** depict the quantified results based on number of migrated cells counted per field. Images were taken by microscope (Olympus-1X73). Scale: 200µm. *p<0.01; **p<0.001 difference between control and treatment.

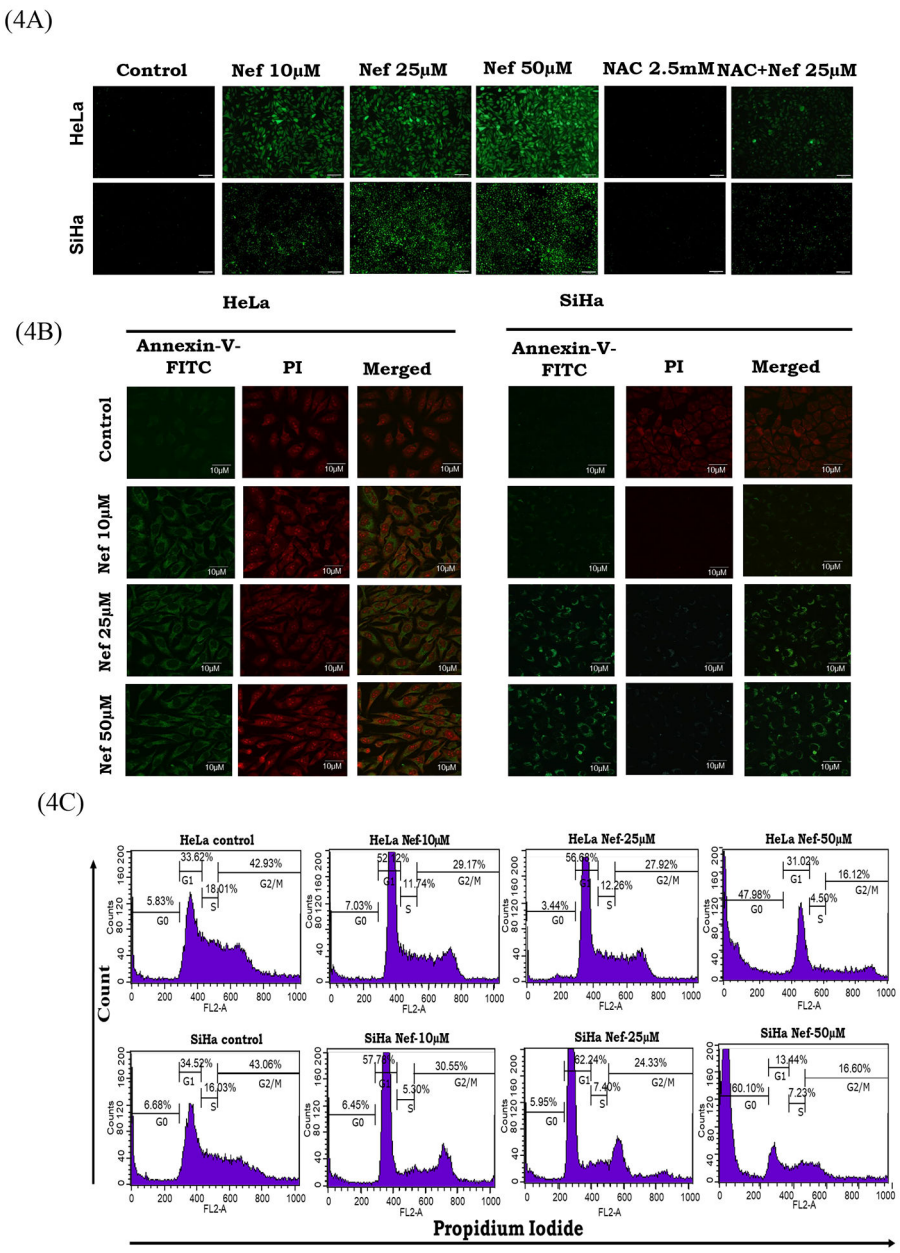

Figure 4: Nef induces oxidative stress in cervical cancer cells.

(A) ROS generation was detected by adding 2',7'-dichlorofluorescin diacetate (DCFDA) fluorescent dye. The fluorescent green color indicated the generation of ROS in Nef (10, 25 and 50μM) treated cells compared to the untreated cells. Conversely, the effect of Nef was abrogated in the presence of antioxidant N-acetyl cysteine (NAC) which resulted in decreased ROS production. (**B) Nef induces apoptosis in cervical cancer cells by Annexin-V-FITC assay.** HeLa (left panel) and SiHa (right Panel) cells were treated with various concentrations of Nef (10, 25 and 50μM) for 48 hrs. Cells were stained with Annexin V-FITC to detect apoptotic cells and PI for nuclear stain. Results showed that Nef induced apoptosis in both HeLa and SiHa cells. **(C) Cell cycle analysis by Flow cytometry:** HeLa and SiHa cells treated with Nef (10, 25 and 50 μM) was subjected to flow cytometry

for cell cycle analysis. Data showed that Nef induced potent G0/G1phase cell cycle arrest in both HeLa and SiHa cells.

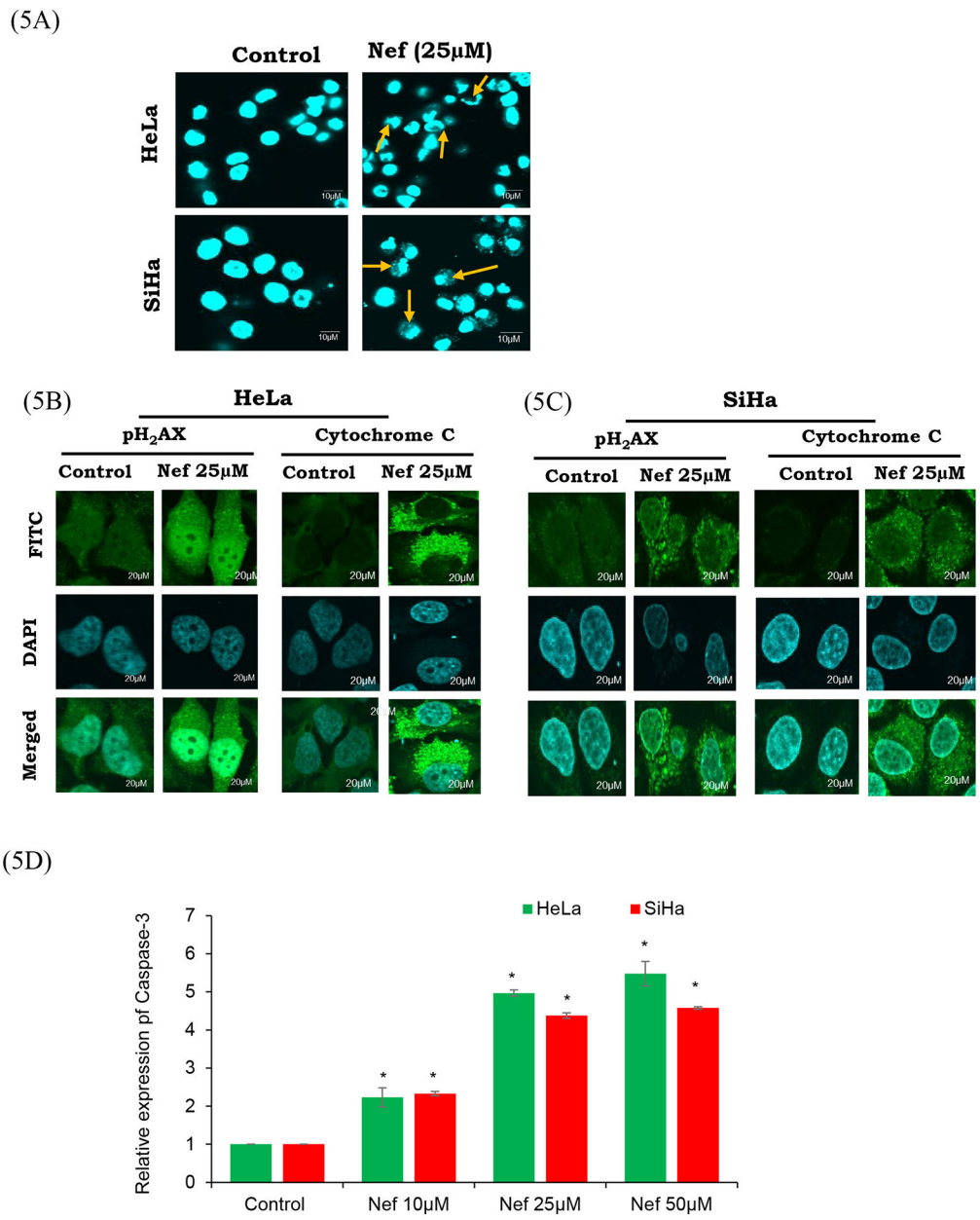

Figure 5: Nef induces apoptosis by activating apoptotic characteristics:

(A) Nuclear morphology of HeLa and SiHa cells stained with DAPI. Apoptotic bodies (arrows), cell swelling, and chromatin lysis were observed. Fluorescence microscopy images are of 60× magnification with scale bar of 10μm. HeLa (**B)** and SiHa **(C)** cells treated with Nef (25μM) were fixed, blocked and probed with pH_2AX and cytochrome-C antibodies. Then the cells were probed with secondary antibody conjugated with FITC (green) and counter stained with DAPI (blue). Nef treated cells showed activation of pH_2AX and cytochrome c compared to untreated control cells. **(D)** Quantitative analysis of relative expression of caspase-3 by ELISA. Both HeLa and SiHa cells treated with Nef show significant increase in the relative expression of caspase-3 in comparison to untreated control

cells. Results are representative of 3 independent experiments. *P<0.01 when compared with the control group.

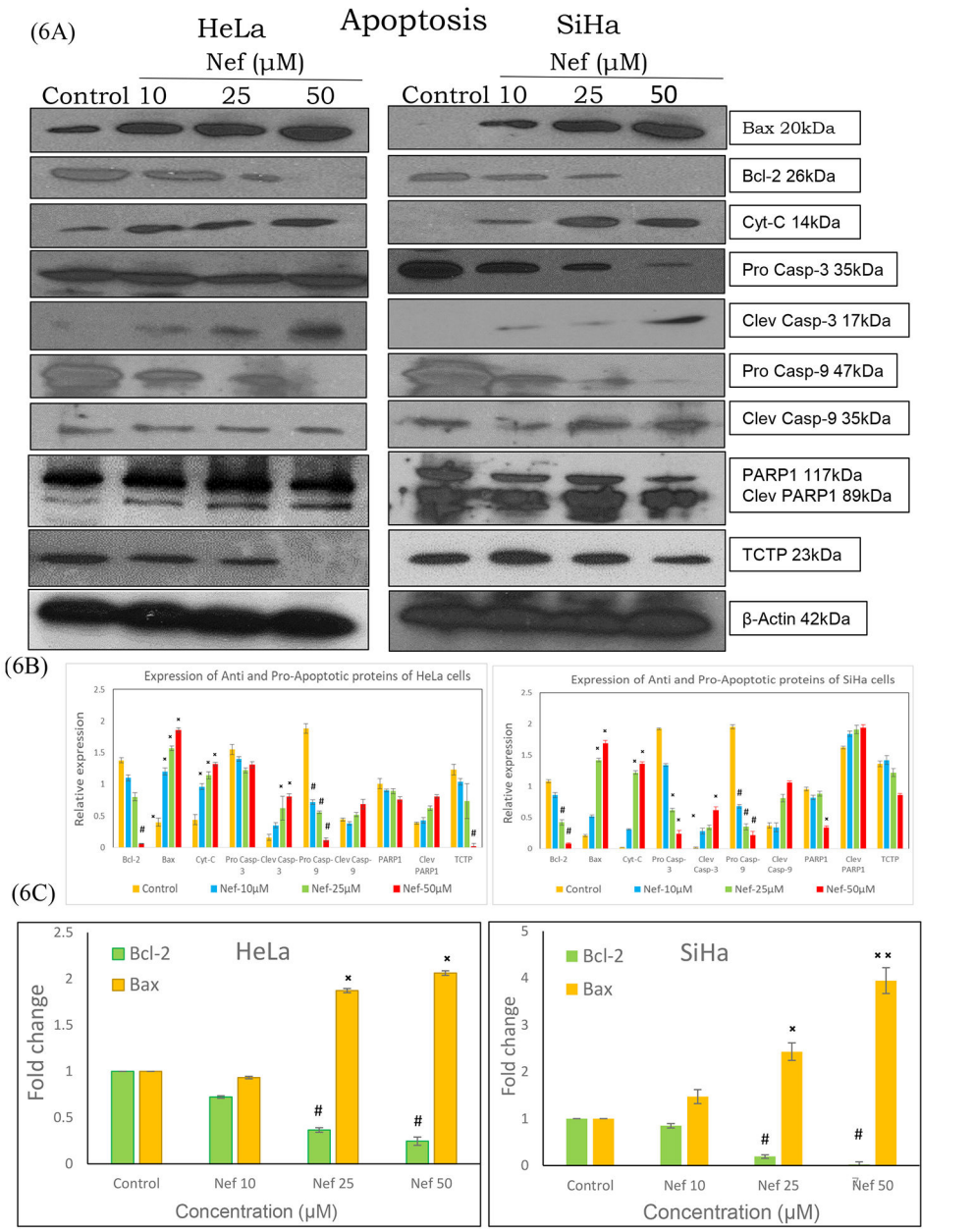

Figure 6:

(A) Western blot and real time-PCR analysis of apoptosis markers in HeLa and SiHa cells. Cell lysates of HeLa and SiHa cells treated with Nef (10, 25 and 50μM) for 48hrs were subjected to SDS-PAGE, transferred to nitrocellulose membrane and probed with respective primary antibodies. Results revealed that Nef treatment increased the expression of pro-apoptotic markers bax, cytochrome c, cleaved caspase-3, −9 and PARP while reducing the levels of anti-apoptotic bcl-2, TCTP, procaspase-3 and −9. Image shown is the chemiluminescent detection of the blots. **(B)** Relative expression of the proteins were normalized using β-actin as loading control and band intensities were quantified using Image J software. *$p < 0.01$ or #$p<0.01$, as compared with the control. **(C)** mRNA expression of bcl-2 and bax was determined by real time-PCR. Results revealed that Nef

upregulated the expression of Bax with concurrent downregulation of Bcl-2. β-actin served as house keeping control in this experiment. Data are representation of one of three experiments. *$p < 0.01$ or #$p<0.01$, as compared with the control.

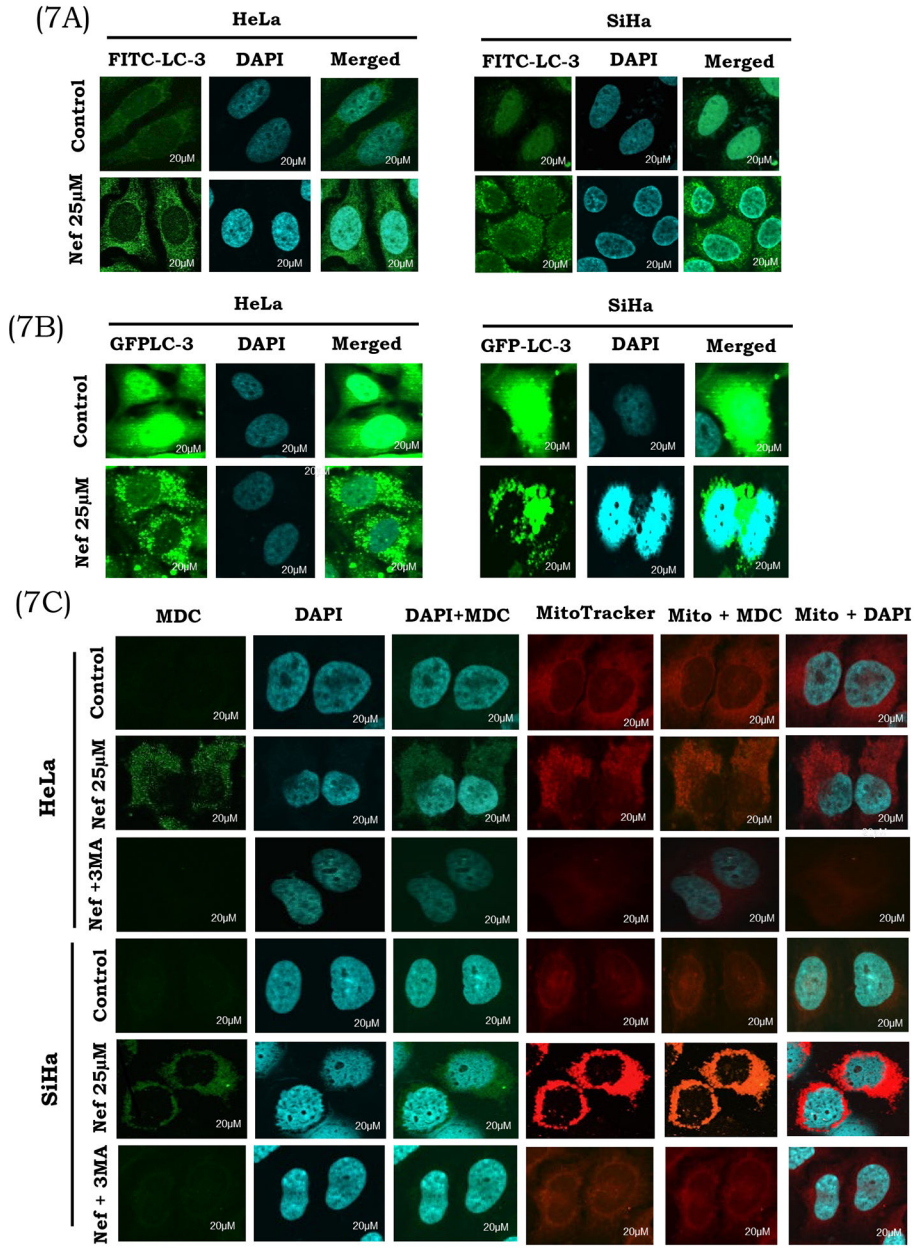

Figure 7: Nef induces autophagy by activation of LC-3:

(A) Nef induces autophagy through the activation of LC-3. Cells treated with Nef (25μM) and autophagy inhibitor 3MA (2.5mM) were analyzed for autophagosome formation using LC3 antibody by immunofluorescence analysis. A massive accumulation of autophagosomes (green fluorescence) occurred in Nef treated HeLa and SiHa Cells. Cells were counter stained with DAPI (blue). **(B)** Nef induces autophagy by GFP-LC-3 activation: Nef induces autophagy through the activation of GFP-LC-3, detected by cells transiently transfected with the GFP-LC-3 plasmid for 4 hrs and treated with Nef (25μM) and autophagy inhibitor 3MA (2.5mM). Detection of GFP-LC-3 puncta from Nef mediated autophagy in both the cervical cancer cells. **(C) Induction of autophagy by Nef in cervical cancer cells:** HeLa and SiHa cells were treated with Nef (25μM) and allowed to incubate for 48hrs. Cells were washed

and probed with MDC (green) and counter stained with DAPI (blue). Cells were also probed with a mitotracker (red fluorescent dye that stains mitochondria). Formation of acidic vesicular organelles was observed by MDC staining in Nef treated cells as compared to control cells. 3MA (2.5mM) was added to cells to block autophagy mediated by Nef. Representative images of cells were taken with a fluorescence microscope at 60X magnification.

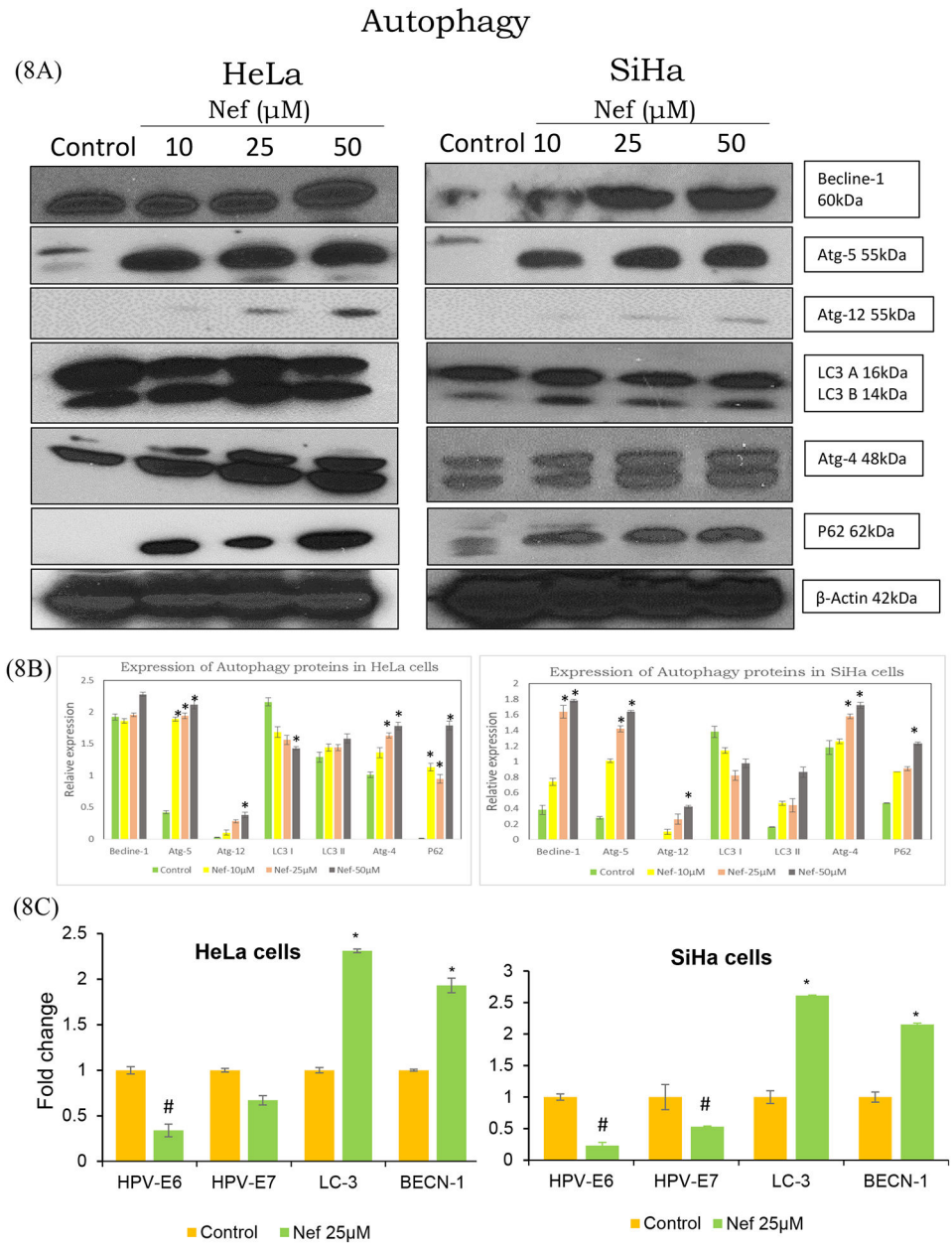

Figure 8:

(A) Autophagy related protein and mRNA expression levels of selected genes in cervical cancer cells treated with Nef: HeLa and SiHa cells were treated with Nef and allowed to grow for 48 hrs, following which cells lysed in protein lysis buffer. Proteins were separated on 10–12% SDS-PAGE and transferred to nitrocellulose membrane, probed with beclin-1, atg-4, 5&12, LC-3 and P62 antibodies. Increased expression of autophagy related proteins, which indicated that Nef induced autophagy in cervical cancer cells. Images shown are the protein bands detected by chemiluminescence. **(B)** Quantitative data of relative protein expression levels as determined by ImageJ software. P<0.01 compared with the control group. **(C)** The mRNA isolated from HeLa and SiHa cells treated with Nef (25μM) was converted to cDNA using High-capacity complementary DNA (cDNA) reverse transcription

kit. Quantification of the expression levels of target genes was conducted using SYBR Green method with both forward and reverse primers. All the transcript levels were normalized using β-actin expression levels. Real time PCR data revealed that HPV early gene (E6 and E7) levels were decreased by Nef treatment compared to untreated controls. On the other hand, Nef increased the expression levels of autophagy specific genes (LC-3, beclin-1) compared to untreated controls. β-actin served as the reference house keeping control. Data are presented as mean ± standard deviation (SD) of three independent experiments. *$p < 0.01$ or #$p<0.01$ compared with the control group.

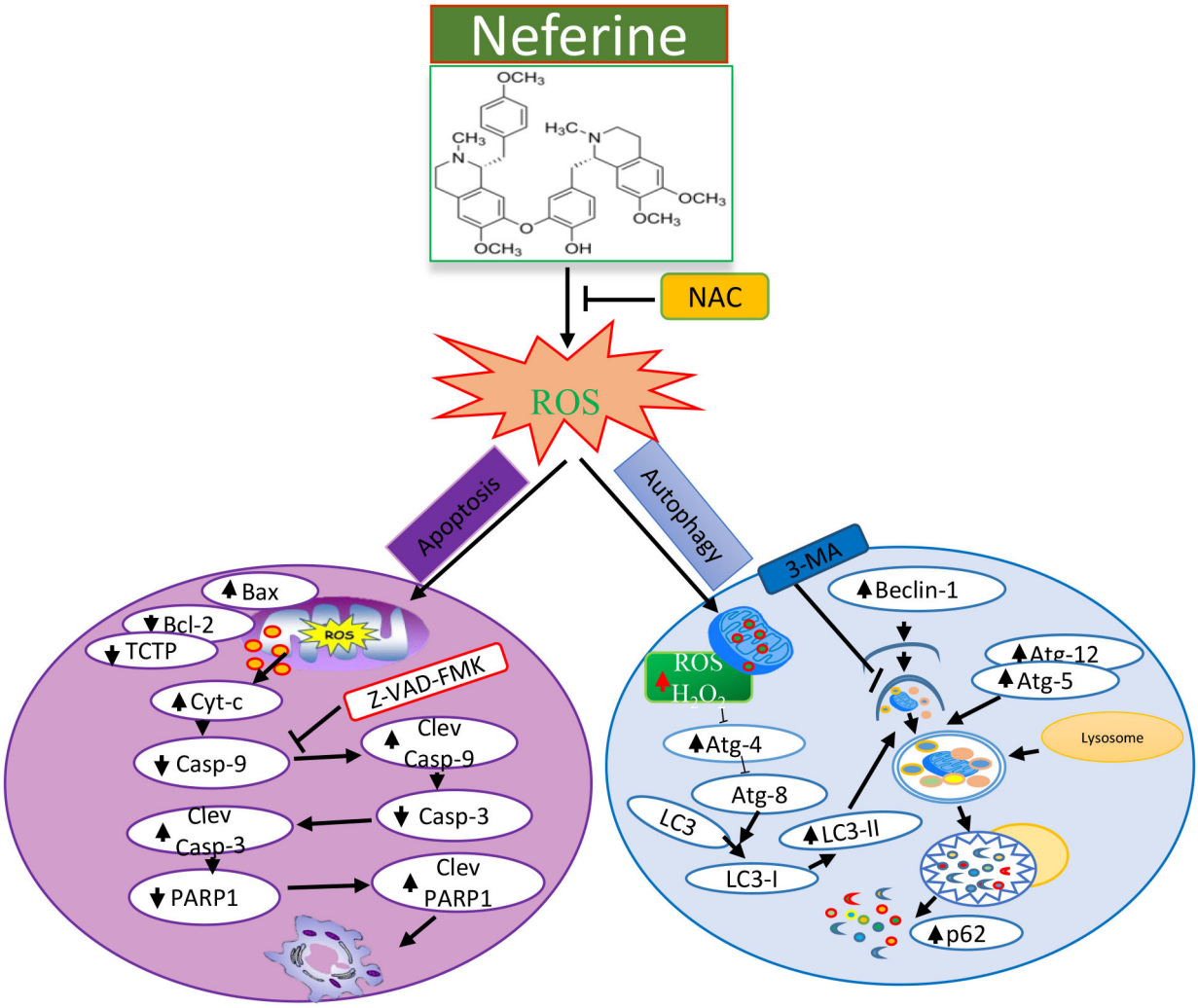

Figure 9.
Schematic mechanisms of Nef-mediated anticancer effects in cervical cancer cells.

Table: 1

Comparison of Nef with other anti-cervical cancer natural compounds

S No	Compound	Source	Cell lines	IC_{50}	Mechanism of Actions	Reference
1	Neferine	*N. nucifera*	HeLa, SiHa	25μM/48hrs	Induces ROS mediated apoptosis and autophagy	Current study
1	Curcumin	Curcuma longa	HeLa	35μM/48hrs	Inhibits the proliferation and invasion through impairing Wnt/β-catenin and NF-kB pathway	Ghasemi et al.,2019
2	PLGA-Curcumin	Curcuma longa	Caski, SiHa	25μM/48hrs	suppressing oncogenic miRNA-21, nuclear β-catenin, and abrogating expression of E6/E7 HPV	Zaman et al.,2016
3	Glycyrrhizin	licorice	HeLa	122μM/48hrs	Induce apoptosis through cycle arrest at G0/G1	Farooqui et al., 2018
4	polysaccharide	Angelica sinensis	HeLa	100μg/ml/ 48hrs	Induces intrinsic apoptotic cell death	Cao et al.,2010
5	Phenanthrenes	*Juncus* species	HeLa	1μM/72hrs	Inducing a G2/M-phase cell cycle arrest and inhibiting cell migration	Kuo et al.,2019
6	Erianin	Dendrobium chrysotoxum	HeLa	32μM/48hrs	induces apoptosis via regulation of the ERK1/2 signaling	Li et al., 2018
7	Emodin	Rheum palmatum	HeLa	100μM/48hrs	Trigger mitotic catastrophe cell death	Trybus et al., 2019
8	Sesquiterpene lactone	Asteraceae	CaSkiSiHa	5.8 & 6.6 μM/24hrs	Induced apoptosis via activation of JNK signaling pathway	Shao et al., 2016
9	RCE-4	Reineckia carnea	HeLa	7μM/24hrs	Inhibiting the PI3K/Akt/mTOR signaling pathway and NF-κB activation	Bai et al.,2016
10	Piperine	Piper nigrum	HeLa	50μM/72hrs	Enhanced the effect to against Paclitaxel-Resistant Cervical Cancer Cells through of Mcl-1	Xie et al.,2019
11	Imperatorin	Angelica dahurica	HeLa	150 μM/ 24hrs	Induce TNF-α-mediated activation of ROS/PI3K/Akt/NF-κB	Wang et al.,2017
12	Protoberberine	Chelidonium majus	HeLa	50μg/ml/ 24hrs	Enhances photodynamic therapy	Warowicka et al.,2019
13	Quercetin	vegetables and fruits	HeLa	100μM/24hrs	Induce cell death via alters the PI3K, MAPK and WNT signaling	Kedhari et al.,2019